Remote Sensing Applications: Society and Environment 11 (2018) 119–139

Contents lists available at ScienceDirect

Remote Sensing Applications: Society and Environment

journal homepage: www.elsevier.com/locate/rsase

Spatio-temporal variations of surface temperatures of Ahmedabad city and its relationship with vegetation and urbanization parameters as indicators of surface temperatures

Aneesh Mathew[a,b,*], Sumit Khandelwal[b], Nivedita Kaul[b]

[a] Department of Civil Engineering, Madanapalle Institute of Technology & Science, Angallu, Madanapalle 517325, Chittoor District, Andhra Pradesh, India
[b] Department of Civil Engineering, Malaviya National Institute of Technology Jaipur, Jaipur 302017, Rajasthan, India

ARTICLE INFO

Keywords:
Land surface temperature
Urban heat island
Enhanced vegetation index
Normalized difference built-up index
Percent impervious surface area
Road Density

ABSTRACT

Land Surface Temperature (LST) has major importance in urban climatology, global climate change, and earth-atmosphere energy transfer. Relationship of vegetation and built-up parameters as indicators of LST has been investigated in the present study. The present study has been carried out to analyze the variations in rising in LST in the urban area than the neighboring rural area for three different seasons' winter, summer and monsoon of the years from 2009 to 2013 using Moderate Resolution Imaging Spectroradiometer (MODIS) sensor data. Analysis of 8-day night-time LST data shows that significant surface urban heat island (SUHI) exists over the Ahmedabad study area. Mean annual SUHI intensity from 2009 to 2013 varies from 6.01 K to 6.56 K, and overall mean SUHI intensity has been found out to be 6.17 K. $SUHI_{index}$ has been used to compare the SUHI intensity of different periods and different seasons. The relationship of LST with normalized difference vegetation index (NDVI), enhanced vegetation index (EVI), road density (RD), normalized difference built-up index (NDBI) and percent impervious surface area (%ISA) has also been investigated in the present work. An inverse relationship has been observed between LST and vegetation indices (VIs) and it is season dependent. EVI has been used as a better vegetation parameter for SUHI studies than NDVI. %ISA has been reported to be a significant parameter for the analysis of SUHI effect and its relationship with LST has been found to be season independent. The relationship between %ISA and LST is similar for all three seasons with a consistent rising trend. A positive relationship has been observed between LST and NDBI especially for monsoon months. The trend of LST-NDBI relationship during different season is different, which indicates that the relationship between LST and NDBI is linear and is season dependent. It has been observed that soil and drier vegetation in rural areas show higher NDBI values. Hence NDBI cannot be used as a good indicator for SUHI studies. %ISA has been found to be a better parameter for SUHI studies compared to NDBI. Another parameter, RD, has been introduced in the present study to represent the extent of urbanization. A consistent positive relationship between RD and LST has been found for all the three study seasons of the entire study period, thus indicating seasonal independence of RD and LST relationship. Use of RD also considers the effect of anthropogenic heat, which is one of the main contributors to the SUHI effect, in addition to the effect of the impervious surfaces. Hence, RD is proposed as a suitable indicator for SUHI studies.

1. Introduction

Human settlements cause modifications in the materials and structures of the Earth surfaces. These changes cause alterations in the energy balance of the surface and the composition of the atmosphere, compared to the surrounding natural terrains. These modifications result in a unique local climate of human settlements, which is called the urban climate and the modification process, is called urbanization. As urban population grows, human development will form into bigger agglomerations of intensely anthropogenic modification of the landscape (Small et al., 2011). The current population growth trajectories show that by 2050, nearly 6.3 billion out of an estimated global population of 9.1 billion (70% of human population) will live in urban areas (United Nations, 2010). Nowadays, an urban city suffers a problem of an urban heat island (UHI) phenomenon where urban areas show higher surface and air temperatures than the countryside due to the surface and atmospheric modifications resulting modified thermal climate in urban areas (Voogt and Oke, 2003; Oke, 1982). UHI refers to

* Corresponding author at: Department of Civil Engineering, Madanapalle Institute of Technology & Science, Angallu, Madanapalle 517325, Chittoor District, Andhra Pradesh, India.
E-mail address: aneesh52006@gmail.com (A. Mathew).

https://doi.org/10.1016/j.rsase.2018.05.003
Received 15 May 2017; Received in revised form 20 May 2018; Accepted 23 May 2018
Available online 26 May 2018

the excess warmth of the urban land or atmosphere compared to non-urbanized surroundings. When land surface temperature (LST) is used for analyzing the UHI effect, it is called surface UHI (SUHI). The difference in air temperatures between urban and their surrounding rural areas is expressed as atmospheric urban heat island (AUHI), which may be divided into two categories: canopy layer urban heat island (CLUHI) for urban canopy layer (layer of urban atmosphere extending from surface to mean building height), and boundary layer urban heat island (BLUHI) for urban boundary layer (layer above canopy layer that is influenced by the underlying urban surface) (Voogt and Oke, 2003). Howard has documented the first instance of UHI as a consequence of urbanization in 1818 (Mirzaei and Haghighat, 2010). In addition to the size of a city, UHI mainly depends on the urban structure, building density, building and road geometry, thermal and optical properties of materials used in urban spar, lack of evaporation in the cities, canyon geometry, surface materials, anthropogenic heat by human activities, vegetation coverage and water bodies in the city (Kovats and Hajat, 2008; Imhoff et al., 2010; Kolokotroni and Giridharan, 2008; Santamouris et al., 2001; Rizwan et al., 2008). Heat stress in urban areas is causing an adverse effect on human health and is expected to worsen in the future due to increase in rapid urbanization by the development of cities and urban expansion and global warming (Rotem-Mindali et al., 2015: Johnson et al., 2012; Kovats and Hajat, 2008; Mathew et al., 2018). Surface UHI has been observed to be largest for neighborhoods with scarce vegetation that have a higher fraction of impervious surfaces, and low albedo values. An increase in the percentage of vegetation cover of 10% drops the surface temperature by 1.3 °C (Klok et al., 2012). Altered surface and air temperature patterns and rise in mean temperatures due to climate change also influence the urban environment resulting UHI effect by altering species habitat (Knapp et al., 2008; Schwarz et al., 2012). UHI affects the local meteorology by changing local wind patterns, increasing humidity, forming cloud and fog and changing the precipitation rate (Taha, 1997).

LST data from various sensors carried by different satellites become available, and a variety of LST related SUHI studies have conducted for different cities (Aniello et al., 1995; Dousset and Gourmelon, 2003; Gallo et al., 1993; Streutker, 2003; Khandelwal et al., 2017), which overcome some problems of in-situ measurements (Hu and Brunsell, 2013). The magnitude of UHI can be expressed in terms of UHI intensity which is the difference between urban and rural temperatures (Clinton et al., 2013; Schwarz et al., 2011). When the difference is positive (urban hotter than rural), there is a SUHI; when the difference is negative, an urban heat sink (SUHS) has been observed. SUHI and SUHS are temporally variable both diurnally and seasonally (Clinton et al., 2013). Strongest UHI has been observed during summer daytime in the Beijing metropolitan region due to the contribution of urban land (Qiao et al., 2013). The spatial extent of the UHI is related to total urban population, and the magnitude of the UHI may be more closely related to urban population density than the overall population (Streutker, 2003). The temperature of a surface is affected by vegetation due to both the cooling effect as well as the shadow effect. However, in urban areas both the vegetation cover and its density is low, and normally it is close to the minimum, and built-up density is maximum to the central business district (CBD) of the city. The large built-up areas and low levels of vegetation are the main reasons of maximum temperature at and around the CBD. Built-up areas are usually well defined in the temperature images and form hot spots (HS). Similarly, cold spots (CS) are characterized by open and vegetated areas and can be regarded as cool islands (Tiangco et al., 2008). Yamashita et al. (1986) have suggested that the UHI intensity tends to increase with increasing city size. The UHI effect is due to the differences in land cover (LC), i.e. difference in the composition of the Earth's surface at rural and urban locations. The altered urban surface normally has reduced evaporating and non-transpiring properties. It has been shown that the partitioning of sensible and latent heat fluxes and thus surface radiant temperature response is a function of changing surface soil moisture and vegetation cover (Owen et al., 1998).

Cheval and Dumitrescu (2009) have reported higher thermal variability during daytime (12.5 °C) than during night time (4.6 °C), in their study on UHI of Bucharest. They have also found that the heat island extends between 5 and 11 km radius from CBD. Tran et al. (2006) have investigated the UHI effects in eight Asian megacities and have found out seasonal variations in the maximum intensity of UHI of Tokyo which is minimum at 3 °C around January-February and maximum at 13 °C around July-August. Similar observations have also been made at other cities of temperate and tropical climates. On the basis of observed air temperature data, the maximum UHI intensity occurs a few hours after sunset, while the most intense UHI can be detected during the daytime when satellite sensor data are used (Roth et al., 1989; Dezső et al., 2005). However, Karl et al. (1988) have suggested that urbanization within the United States exerts its greatest impact on minimum (compared to maximum or mean) temperature (which is mainly a nocturnal phenomenon) and have found that the UHI effect is most significant during the night. All these observations indicate that not only the UHI intensity is highly variable, but any generalization about its behavior may not be universally applicable. Borbora and Das (2014) have reported the existence of summer UHI above 2 °C in Guwahati City, India with highest magnitude of daytime and nighttime UHI Intensity (UHII) of 2.12 °C and 2.29 °C, respectively.

Vegetation cover is one of the most readily controllable variables in urban landscapes and is the primary target for intervention strategies to mitigate SUHI effect (Clinton et al., 2013; Jonsson, 2004). Previous research shows that vegetated areas show lower surface temperatures than impervious ones (Owen et al., 1998). LST, skin temperature of the Earth surface, is one of the most important parameters for analyzing UHIs (Aguiar et al., 2002; Ma et al., 2010; Mallick et al., 2012; Sobrino et al., 2012). LST has significant negative correlations with the normalized difference vegetation index (NDVI) (Liang and Weng, 2011; Tran et al., 2006; Mackey et al., 2012a, 2012b; Deng et al., 2013; Chen et al., 2006; Guo et al., 2015; Yue et al., 2007; Gillies et al., 1997; Weng et al., 2004; Dousset and Gourmelon, 2003; Gallo et al., 1993; Qiao et al., 2013; Alshaikh, 2015; Mathew et al., 2017a) as well as fractional vegetation cover (Fv) through vegetation indices (Wu et al., 2014; Li et al., 2012; Weng et al., 2004), while LST positively correlates to impervious surface area (Dousset and Gourmelon, 2003; Lazzarini et al., 2012; Wilson et al., 2003; Yuan and Bauer, 2007; Mathew et al., 2016; Deng et al., 2013; Chen et al., 2006; Xiao et al., 2007; Xian and Crane, 2006; Civco et al., 2002; Zhang et al., 2010). ISA has been found to be one of the primary drivers for rising in temperature explaining 70% of the total variance in LST (Imhoff et al., 2010). Percent ISA, combined with LST, and NDBI, can quantitatively explain the spatial distribution and temporal variation of urban thermal patterns and associated land use/land cover (LU-LC) conditions (Zhang et al., 2009). Li et al. (2012) have observed that surrounding rural areas show lower LSTs and relative lower variation in LSTs than urban areas. Also, significant relationships between LST and Fv, population density, and road density have been observed. Urban land surfaces strongly influence LST and its spatial heterogeneity within UHI. NDVI and NDBI are well correlated with the changes of LST whereas normalized difference bareness index (NDBaI) has a weaker correlation with LST (Guo et al., 2015). The NDBaI that represents soil distribution in urban areas, showing a negative relationship with LST (Chen et al., 2006). Positive correlation has been observed between LST and NDBI in many studies (Deng and Wu, 2013; Chen et al., 2006; Pal and Ziaul, 2016; Zhang et al., 2009; Mathew et al., 2015; Guo et al., 2015). Remote sensing based urban surface biophysical composition such as vegetation abundance, impervious surface, water bodies and soil fractions have been found to be the best indicators of surface temperature variations across space (Deng and Wu, 2013; Xiao et al., 2007; Zhang et al., 2009; Guo et al., 2015). Changes in LU-LC, urban sprawling, and population shifts resulted in significant variation in the spatiotemporal patterns of the UHIs due to

the destruction of different water features and vegetated surfaces (Zhang et al., 2013). Intensive and rapid urbanization is an illustration of human-induced LU-LC change, which has worsened the ongoing impacts on the climate system by changing the thermal pattern (Jin et al., 2005). Variations in LU-LC conditions significantly influence the climatological diurnal temperature range (Gallo et al., 1996; Mathew et al., 2017b). Spatial variation of NDVI is not only subject to the effect of vegetation, but also to topography, elevation, slope, availability of solar radiation, and other factors (Walsh et al., 1997).

EVI is also a vegetation index, and it is different from NDVI due to the use of parameters for the reduction in atmospheric influences (Huete et al., 1999). Since the improvements of EVI over NDVI, it is required to explore its application for UHI studies. The MODIS EVI product is calculated from atmospherically modified bi-directional surface reflectance that has been masked for water, heavy aerosols, clouds, and cloud shadows. EVI reduces canopy background variations and maintains better sensitivity over dense vegetation conditions. EVI also uses the blue band to exclude residual atmosphere contamination generated by smoke and sub-pixel thin clouds (Huete et al., 1999).

Ahmedabad city features the fastest growing cities in the world. The projected growth rate of Ahmedabad city is much higher than the corresponding rate of other big metropolitan cities of India. The high growth rate will cause a lot of burden on the city infrastructure, and large-scale development will be required for the increased population. If in addition to various principles of planning, the information available on UHI is also utilized during the process of development, it may enable the city planners to design the physical urban layout in such a manner that it helps to contain UHI associated with the development. Hence, a better understanding of the heat island effect and its relationship with the urban landscape parameters is required, for more efficient city planning. In the present times, when the entire world is reeling under the impacts of climate change, studies of such nature might prove to be helpful in generating substantial knowledge about the UHI phenomenon which might be further used in developing strategies for mitigating its effects on the global climate. The proposed research is a step towards increasing the understanding of the UHI and the factors responsible for it. The study will also help in the quantification of the effect of these factors on UHI. India has witnessed unprecedented development in recent past and due to that many Indian cities have developed at a rapid pace. The aim of the current research is to enhance the understanding of the effects of LST and various parameters on spatial and temporal patterns of UHI, with a case study of Ahmedabad city in India. The study has been carried out to analyze the UHI effect over Ahmedabad city and to find the SUHI intensity over the city for different seasons. The objective of the present study is to investigate the effect of vegetation and urbanization on LST, using NDVI and EVI as vegetation parameters and %ISA, road density (RD) and NDBI as urbanization parameters.

2. Study area: Ahmedabad City

Ahmedabad city was chosen as the study area, the former capital of the state of Gujrat, which is the biggest city in the state located on the banks of Sabarmati river. It is the fifth largest city and seventh largest metropolitan area of India with a human population of higher than 5.8 million and an extended population of 6.3 million. According to the census of 2011, the urban population of Ahmedabad city was 6,352,254. Ahmedabad is situated on 23° 09' 54.68"N 72° 33' 40.02"E and 22° 54' 19.90"N and 72° 39' 51.62"E according to the geographic coordinate system. Fig. 1 shows the geographical location of the study area. Ahmedabad has a hot semi-arid climate with scanty rainfall throughout the year. The weather is warm from March to June during the summer season with mean maximum and minimum temperature of 42 °C and 27 °C, respectively. Winter season from November to February experiences cold weather with mean maximum and minimum temperature of 30 °C and 15 °C, respectively. Monsoon season from July to October experiences wide fluctuations in daily average air temperature due to atmospheric conditions. The study area is mostly water scarce with average annual rainfall of approximately 800 mm concentrated mostly during the monsoon season. According to Köppen and Geiger, the climate of Ahmedabad city is classified as BSh, hot steppe climate (semi-arid) with marginally less rain than required for a tropical savanna climate. Kankaria and Chandola lakes located in the southern part of the city, play a vital role in regulating the temperatures during hot summer days. Sabarmati riverfront exists in between the center of the city also contributes much towards cooling of the city.

As UHI phenomenon indicates a warmer thermal climate of urban land, compared to a rural area, the study area must include sufficient rural/suburban area outside the urban area for UHI studies. The boundary of the urban area of Ahmedabad city has been obtained by extracting urban area polygon from the MODIS yearly land cover (LC) type image (MCD12Q1) of 2011. The urban area polygon from this map has been automatically generated by using raster to polygon conversion tool in ArcGIS. The size (length and width) of urban area polygon (hereafter referred to as an urban boundary) are around 12 km and 17 km, in the North-South and East-West direction, respectively.

The urban boundary is enclosed by a buffer of 5 km to mark the boundary of the study area to avoid the influence of Gandhinagar city, and the study has been carried out for area falling within this boundary. The study area covers approximately 750 km^2. The raster pixel size of LST product is 926.6 m, and LST image of the study area has 804 pixels. Fig. 2 shows the Google Earth© image of the study area and urban area of Ahmedabad city.

3. Data and methodology

Eight day, 1 km MYD11A2 land surface temperature and emissivity product of MODIS Aqua and 16 day, 231.7 m MYD13Q1 vegetation product of overlapping dates have been used for the present study. The land surface temperature and emissivity product are available with a quality flag which has been checked to include only the high-quality pixels in the analysis. Landsat Thermal Mapper (TM) and Operational Land Imager (OLI) sensor images have also been selected for the present study for their better imaging quality (Table 1).

The Landsat images have been geometrically corrected to the UTM projection system (datum WGS 84, Zone 43). The ground control points have been selected in order to make sure that RMS error lies below 0.5 pixels. A second-order polynomial and the nearest neighbor resampling method have been employed for implementing the geo-rectification. The digital numbers of the OLI/TM images have been converted to the exoatmospheric reflectance using the methods provided by the Landsat science data user's handbook.

Downloaded MODIS images have been preprocessed using MODIS Reprojection Tools (MRT). Subsetting of the MODIS data to a smaller area has also been done using MRT tools. The data has also simultaneously been re-projected from Sinusoidal projection to UTM Zone 43N projection system with WGS 84 datum and has been reformatted from HDF-EOS to GeoTIFF format.

Linear spectral mixture analysis (LSMA) method has been used for the extraction of impervious surfaces using ENVI 5.0 software. Landsat-derived %ISA layers are approximately at 30 m ground resolution, whereas MYD11A2 product for Night LST has a resolution of approximately 926.6 m. In order to compare %ISA with LST, it is essential for both of them have same resolution so that %ISA layers have been aggregated to the same resolution as of LST layer and they have also been snapped to LST image.

3.1. Calculation of SUHI magnitude

The magnitude of SUHI can be expressed in terms of intensity which is the difference between urban and rural LST (Clinton and Gong, 2013).

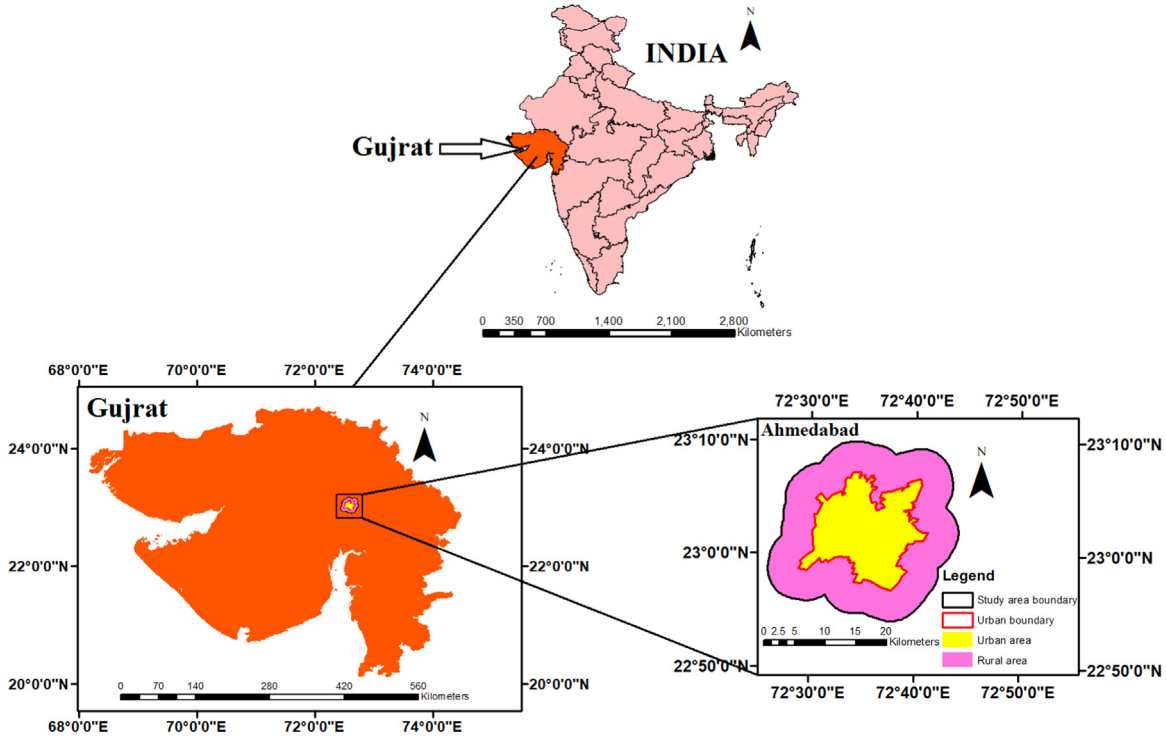

Fig. 1. Ahmedabad Study Area.

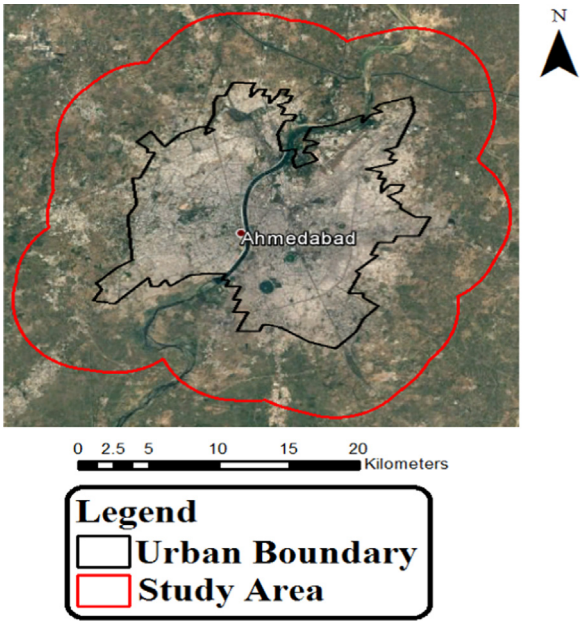

Fig. 2. Google Earth© image of the Ahmedabad study area.

$$\text{SUHI intensity} = LST_{urban} - LST_{rural} \quad (1)$$

SUHI intensity is calculated as the difference in temperature between two points, within the area of interest, during simultaneous observations. SUHI intensity when recorded on the basis of maximum and minimum temperatures, it is called maximum SUHI intensity.

3.2. Derivation of NDVI, EVI, and NDBI

NDVI and EVI have been used to identify vegetation cover in the study area. NDVI is a measure of the amount of vegetation at the surface (Kumar et al., 2012; Purevdorj et al., 1998). The value of NDVI varies between − 1 and + 1. NDVI can be calculated by the following equation (Holme et al., 1987).

$$NDVI = NIR–RED/NIR + RED \quad (2)$$

where, RED = Spectral Reflectance acquired in Red; NIR = Spectral Reflectance acquired in Near Infrared.

EVI can minimize the atmospheric influences and has a soil adjustment factor also. It is computed by Eq. (3),

$$EVI = 2 * \frac{(\rho_{NIR-} \ \rho_{Red})}{(L+\rho_{NIR} + C_1\rho_{Red} - C_2 \ \rho_{Blue})} \quad (3)$$

where, ρ is 'apparent' (top-of-the-atmosphere) or 'surface' directional reflectance, L is a canopy background adjustment term, and C1 and C2 weigh the usage of the blue channel in the aerosol correction of the red channel (Huete et al., 1994)

NDBI has been used to extract built-up areas. NDBI is sensitive to the built-up areas, and it can be determined by the following equation (Zha et al., 2003, Liu and Zhang, 2011).

Table 1
Remote sensing data used for the present work.

Remote Sensing Product	Short Name	Sensor	Platform	Temporal Resolution	Spatial Resolution (m)
Land Cover Type	MCD12Q1	MODIS	Combined Aqua & Terra	Yearly	463.3
Land Surface Temperature and Emissivity	MYD11A2	MODIS	Aqua	8 Day	926.6
Vegetation Indices	MYD13Q1	MODIS	Aqua	16 Day	231.7
Various Bands	–	TM/OLI	Landsat	16 Day	30

$$NDBI = SWIR - NIR/SWIR + NIR \quad (4)$$

where, NIR = Near Infrared Reflectance; SWIR = Shortwave Infrared Reflectance.

3.3. Calculation of Road Density (RD)

Road density (RD) has been calculated as the length of roads per unit area. Unit of RD is km/km^2.

Road network map of Ahmedabad study area has been created by on-screen digitization of the roads from Google Earth. All the roads, major or minor have been digitized within the study area. This roadmap has been used for calculating RD by line density tool in the spatial analyst toolbox using the ArcGIS© software. Line density is calculated as magnitude per unit area of the feature that falls within a defined radius using centroid of the pixel as the center of the circle. Pixel of size 926.626 m inscribed in a circle whose radius has to be determined for line density calculation. When pixel inscribed in a circle, the radius of the circle has been calculated by (√2*side of the pixel)/2. Here pixel size is 926.626 m. Hence the radius of the circle is 655 m as per the equation. As the pixel size of LST is 926.626 m, the radius for calculating RD has been taken as 655 m. The area of the circle considered for calculating RD of a pixel is 57% more than the area of the corresponding pixel.

4. Results and discussion

4.1. LST pattern and SUHI intensity of Ahmedabad city

LST analysis of Ahmedabad city has been done for five years (2009–2013) on a season basis. The total number of 193 MODIS LST scenes of 5 years from 2009 to 2013 have been used in the present work for SUHI analysis. The entire year is divided into winter, monsoon and summer season and the LST and SUHI analysis have been done seasonally. Retrieval of LST of the study area has been done using remote sensing data and GIS techniques. Fig. 3 shows the 8 day LST images of the study area for summer, monsoon and winter seasons of different periods. LST of the urban area shows higher values as compared to the area outside the urban boundary, and most of the pixels representing higher temperature are within the urban boundary. The effect of low-built up density of an area on LST can be clearly understood by analyzing non-urban zone with the urban zone, as the temperature of the non-urbanized zone is lower as compared to the LST of the area within the urban area. The red color in Fig. 3 indicates high temperature in the central part of the city, and light bluish color shows the low temperature at the periphery of the study area which comes under the rural belt, the temperature is low in the countryside because of green vegetation. Urban areas show higher temperature pixels due to the presence of impervious surfaces like built-up areas and anthropogenic materials in the urban areas compared to rural areas. The pattern of LST for the entire study area, as a whole, does not change significantly throughout the year. It can be seen from the images that LST of the urban area is higher than the LST of the non-urbanized area, thus indicating the existence of a clear SUHI over Ahmedabad city. Out of all the three seasons, winter LST map shows noticeable SUHI effects with a clear contrast in temperature of the urban area and the rural area.

Absolute maximum LST for the summer season is found to be 304.2 K and the absolute maximum LST values for winter and monsoon season are 298.78 K and 301.38 K, respectively. Similarly, absolute minimum values of LST for summer, monsoon and winter season are 285.46 K, 285.42 K, and 281.26 K, respectively.

LST of different parts of a city shows both spatial and temporal variations. SUHI intensity has been described as the difference in temperature between two points, within the area of interest (study area in this case), during simultaneous observations. SUHI intensity has been referred to as maximum SUHI intensity corresponding to pixels/points observing the maximum and minimum temperatures. Maximum and minimum LST values of 193 scenes have been recorded for seasonal and annual SUHI intensity calculation.

SUHI intensity exhibits diurnal and seasonal variations and is affected by meteorological conditions, such as cloud, wind conditions as well as anthropogenic heat release. Table 2 gives the average SUHI intensity during different seasons of the study period. Significant SUHI exists over the study area, and high SUHI intensity has been observed during many periods every year. Overall maximum SUHI intensity has been recorded as 11.22 K during the monsoon season of 2011. For the study duration between 2009 and 2013, the maximum SUHI intensity of the study area during different seasons varies from 5.20 K to 11.22 K. Similarly minimum SUHI intensity during different seasons varies from 2.22 K to 6.56 K. The maximum SUHI intensity varies from 8.32 to 8.78 K during summer season and 7.48–11.22 K during monsoon season and 8.72–10.02 K during winter season. Similarly, minimum SUHI intensity varies from 2.46 to 3.28 K, 2.22–4.04 K, and 4.22–6.56 K for summer, monsoon and winter season, respectively. It has been found out that raining during monsoon season increases the moisture content in the soil so that it absorbs more heat during daytime and temperature of that kind of environment will increase so that sometimes LST is more during monsoon season in the rural area or villages around the Ahmedabad city. Average SUHI intensity of different seasons varies from 4.68 K to 7.40 K. Overall average SUHI intensity of the study area during monsoon, summer and winter seasons is 5.38 K, 6.06 K, and 7.07 K, respectively. Overall average SUHI intensity of the study area for all seasons is 6.17 K.

The maximum and minimum temperatures for different periods of different years are highly variable, depending on the season of the year. Similarly, the SUHI intensity at a particular area also varies considerably. Due to these reasons, comparison of SUHI intensity at a particular location or SUHI intensity of various locations during different time periods is very difficult. Further, it is impossible to estimate the consolidated SUHI effect over the entire study area from the LST data of an extended period. To facilitate such calculations, LST values of all pixels of an image have been normalized between 0 and 1, using $SUHI_{index}$. $SUHI_{index}$ has been computed as

$$SUHI_{index} = (LST_i - LST_{min})/(LST_{max} - LST_{min}) \quad (5)$$

where, LST_i is the LST of the pixel for a particular image, LST_{max} is the maximum value of LST over the study area, LST_{min} is the minimum value of LST over the study area.

Maximum and minimum temperatures have been fixed based on the road density (RD) and %ISA values. Maximum temperature pixel has been fixed as the pixel having a maximum RD value of 39.44 km per square km and %ISA of 100%, located at the central part of the urban area which is a part of CBD. Similarly, minimum temperature pixel has been fixed as the pixel having a minimum RD and %ISA value of zero, located in the rural area near study area boundary where vegetation density is higher.

SUHI intensity over a city is calculated on the basis of simultaneous maximum and minimum temperatures recorded at any two places of a city. These temperatures are highly variable, and thus the SUHI intensity also undergoes considerable temporal and seasonal variations. It is a well-known fact that the maximum temperatures at any time are usually observed at one or other part of CBD. The minimum temperatures at the same time are usually observed at the suburban or rural locations, and this location can be anywhere on or near the outer boundary of the area of interest, depending on a variety of meteorological or other parameters. If these variable temperatures are used for finding the average SUHI effect of a city, it can bring reasonable inaccuracies owing to the bias introduced by few abnormally higher/lower temperatures.

$SUHI_{index}$ of all the pixels of the study area has been calculated for the entire study period (193 images of 5 years from 2009 to 2013), and an average of the $SUHI_{index}$ of all the images has been calculated. Fig. 4

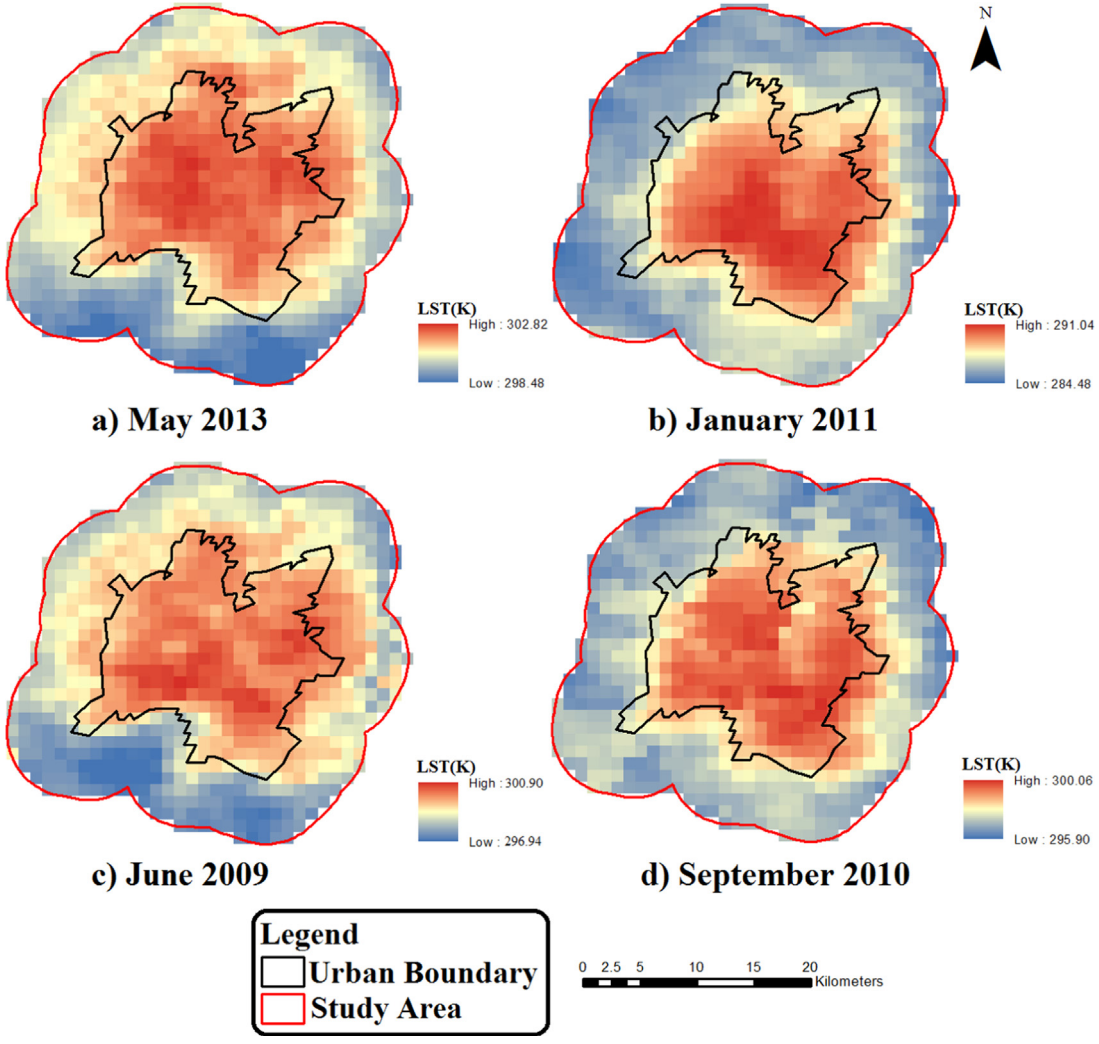

Fig. 3. LST images for different seasons.

Table 2
Average SUHI intensity (K) during different seasons.

SEASON	2009	2010	2011	2012	2013	Overall Average
Summer	5.955	6.228	6.088	5.916	6.127	6.063
Monsoon	4.678	5.387	6.533	5.022	5.287	5.381
Winter	7.398	6.754	7.065	7.155	6.978	7.070
Annual	6.010	6.123	6.562	6.031	6.130	6.171

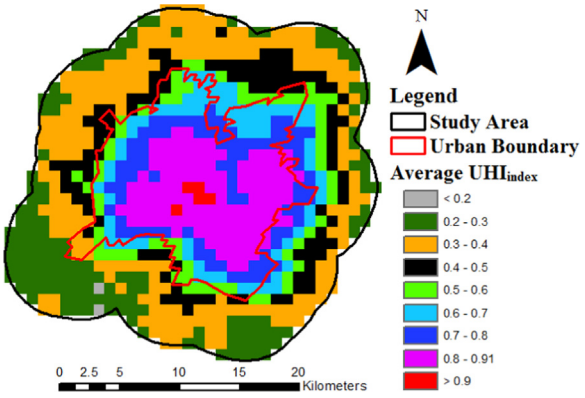

Fig. 4. Average $SUHI_{index}$ image of the study area.

shows the average normalized SUHI intensity ($SUHI_{index}$) over the study area. The maximum value of average $SUHI_{index}$ is 0.93, and all the five pixels in red color in Fig. 4 correspond to the average $SUHI_{index}$ value of more than 0.90. These pixels which are the part of the CBD of Ahmedabad city, are the center of the urban heat island. Other high-temperature pixels are placed around these pixels.

The urban area has only high-temperature pixels and the minimum value of average $SUHI_{index}$ in the urban area is 0.31 and mean of average $SUHI_{index}$ of the urban area is 0.71. Similarly, the maximum and minimum values of average $SUHI_{index}$ corresponding to the rural area are 0.81 and 0.16, respectively. The minimum average $SUHI_{index}$ value of 0.16 indicates that minimum temperature pixels of the entire study area are not same during different periods. Mean of average $SUHI_{index}$ corresponding to the rural area is 0.37. The overall temperature pattern is similar to that discussed earlier, and the $SUHI_{index}$ can be conveniently used for comparison of SUHI intensity at a particular location during different periods or SUHI intensity of different locations during different periods.

The relationship of LST with EVI, NDVI, NDBI, %ISA, and RD has been analyzed in the following sections. Pixels fulfilling the quality criteria discussed earlier for LST, and different parameters have only been used. Though the study area has 804 pixels, some pixels have been eliminated as they do not fulfill the predetermined quality criteria. It can be observed that during summer and winter season, most of the pixels of the study area fulfill the quality criteria. However, due to cloud cover, atmospheric and other effects, a large number of pixels

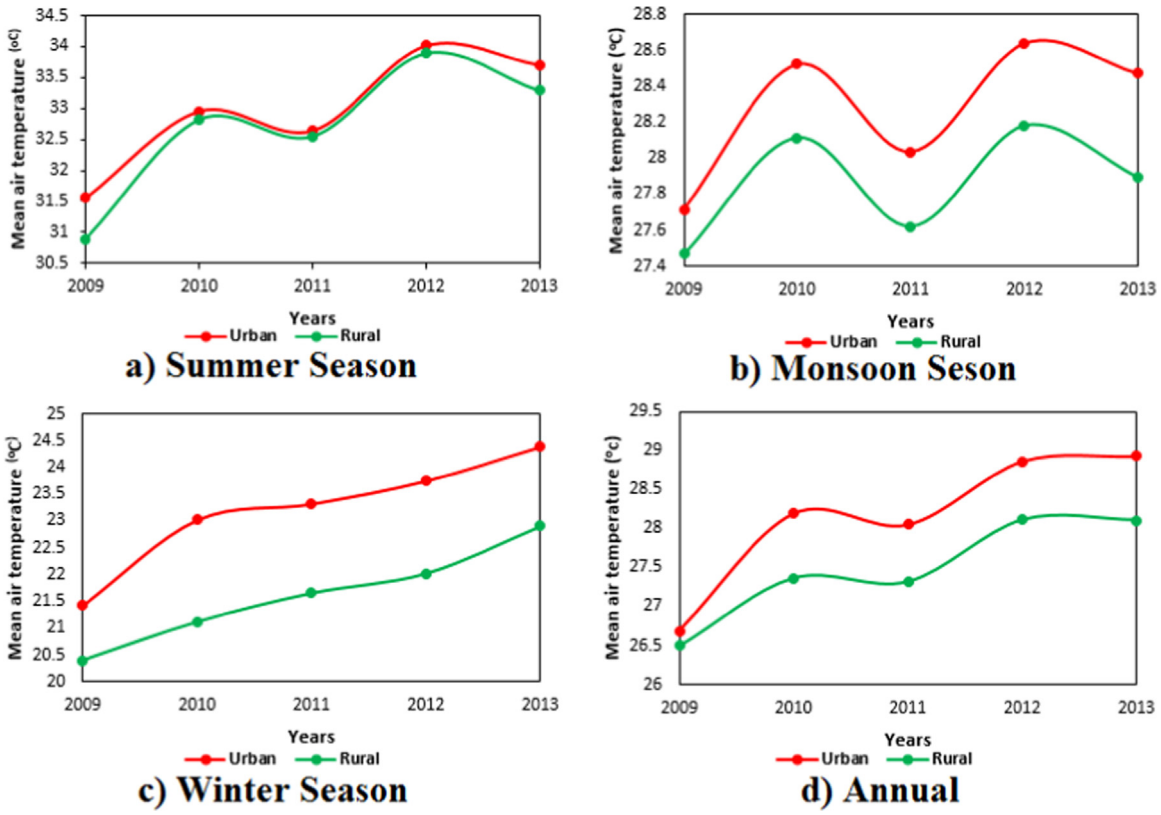

Fig. 5. Temporal mean air temperature variations in urban and rural areas.

have been eliminated during different periods of the monsoon season.

4.2. Atmospheric urban heat island (AUHI) pattern of Ahmedabad city

AUHI pattern has also been studied over the study area for different seasons using the ground meteorological network data (Meteorological Centre, Ahmedabad) and it has been observed that significant AUHI exists over the study area. AUHI analysis of Ahmedabad city has been done for five years (2009–2013) on a season basis. AUHI intensity has been calculated as a difference between mean air temperature in the city area and the rural area. Mean AUHI intensity for different seasons varies from 0.10 °C to 1.91 °C. The overall average AUHI intensity of the study area during summer, monsoon and winter seasons is 0.29 °C, 0.42 °C, and 1.57 °C, respectively. The overall average AUHI intensity of the study area for all seasons is 0.67 °C. The AUHI intensity varies from 0.10 °C to 0.67 °C during the summer season and 0.25–0.58 °C during monsoon season and 1.04 °C to 1.91 °C during the winter season. Strong and weak AUHI has been observed during the winter season and summer season, respectively. Fig. 5 shows the temporal mean air temperature pattern of the study area for different seasons. The observation shows a clear picture of the existence of AUHI for the summer, monsoon and winter season, making urban area hotter than surrounding non-urbanized areas.

4.3. Pattern of vegetation indices

LST mainly depends on nature of LU-LC which ranges from bare soil to vegetation of variable density. Vegetation index (VI) is used to represent the intensity of vegetation over an area. The study area has semi-arid climate and rainfall during monsoon season and groundwater are the primary sources of fulfilling water demand. Vegetation and agriculture, throughout the study area, mainly depend on monsoon rainfall, and hence vegetation density is different during same periods of different years. In order to analyze the seasonal and spatial pattern of VIs over the study area, 16-day NDVI and EVI images of different periods, representing three seasons, starting from 2009 to 2013 have been used for the present study. NDVI and EVI images of different periods, representing three seasons of years 2009, 2010, 2011, and 2013 are shown in Figs. 6 and 7.

Fig. 6 corresponds to NDVI images of the study area of different seasons. Frequent spalls of rainfall during monsoon results in the growth of vegetation of variable density over the entire study area. Poorly vegetated areas have lower VI values and appear purple while highly vegetated areas appear green in the Figs. 6 and 7. Rural area has very few purple spots and different intensity green spots indicating varying vegetation growth. Sowing is done before the monsoon season, and the agricultural fields throughout the study area contribute towards the VI values. The center of the urban area shows much darker purple and represent much lower NDVI values, in comparison to other parts of the urban area which appear light purple. A large percentage of these areas comprises of the impervious built-up surface, and there is very little (almost insignificant) vegetation on these regions. A large portion of the urban area appears purple as there is less scope of vegetation growth due to urbanization. Fig. 7 shows a similar trend in EVI image. EVI values are usually lower than the NDVI values, due to improvement in EVI calculations. There is a continuous reduction of green color throughout the study area from March to May, and very few isolated patches of vegetation can be seen. High temperature and low supply of water during summer season cause degradation in the density of vegetation of the study area. The range of VI values is lowest during the summer months.

The range of VI values is more during winter season than the monsoon season. Vegetation in the urban area is significantly lower during winter season compared to monsoon season (Figs. 6 and 7). Sowing of Rabi crop is normally done during October-November, and the effect of crop growth can be seen in the VI images from December to February, in which there is a continuous increase in VI values of the rural area, whereas the VI values of urban area decrease regularly.

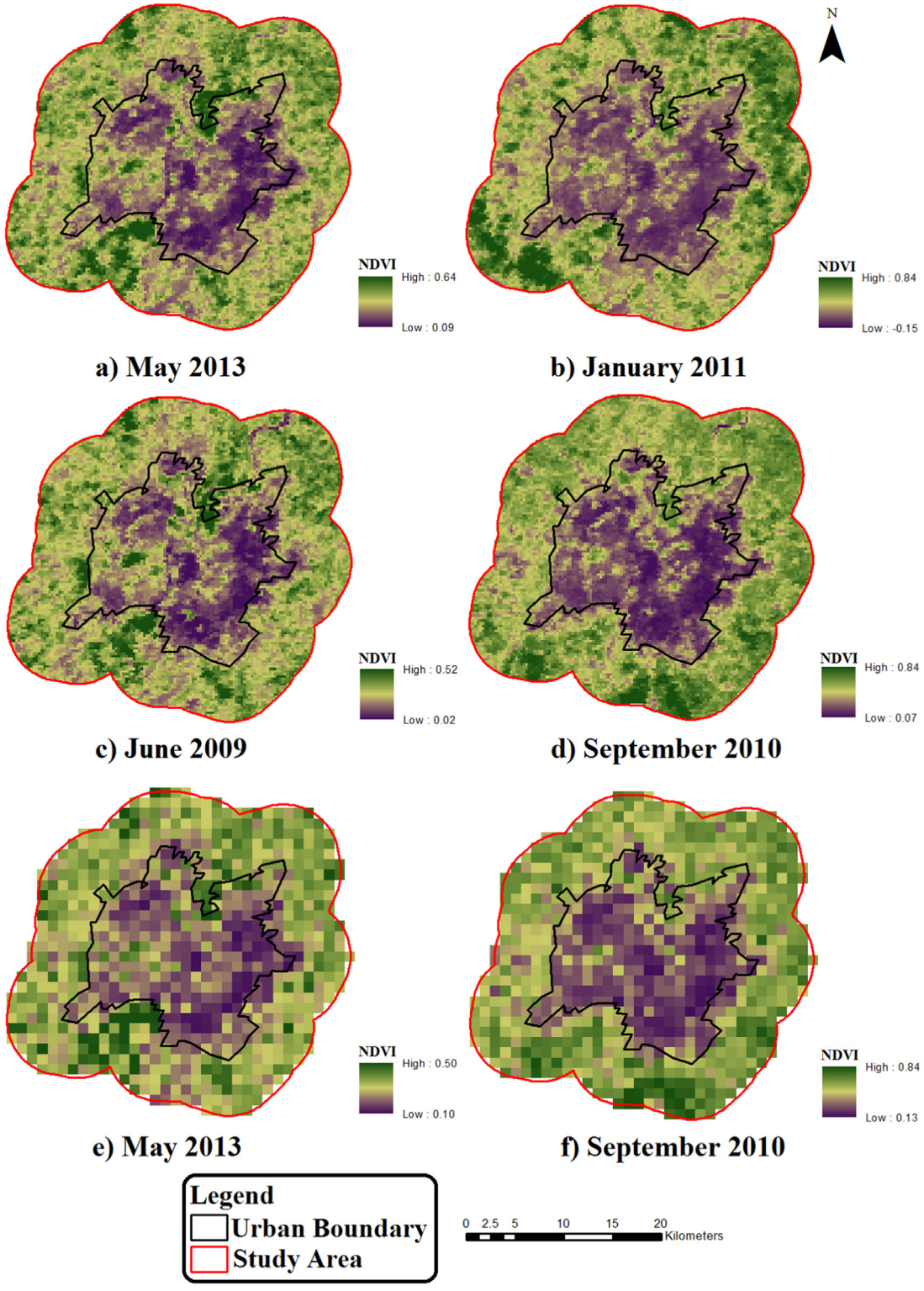

Fig. 6. NDVI images of the study area for different seasons.

Harvesting of Rabi crop is done from March and continues up to May. There is a continuous reduction of green color throughout the study area from March to May, and very few isolated patches of vegetation can be seen. High temperature and low supply of water during summer season cause degradation in the density of vegetation of the study area. The range of VI values is lowest during the summer season. A Large part of the study area is dark purple during the summer season, and VI values are typically for barren land. Few localized green spots are visible both inside and outside the urban boundary. Kharif season starts with some pre-monsoon showers in May-June and sowing is done after that.

Mean values of VIs is minimum during the summer season and maximum during the monsoon season. EVI values are usually lower than the NDVI values, due to improvement in EVI calculations. Due to the aggregation of VI pixels, there is some reduction in the maximum value of VI whereas the minimum values of VI increases due to this

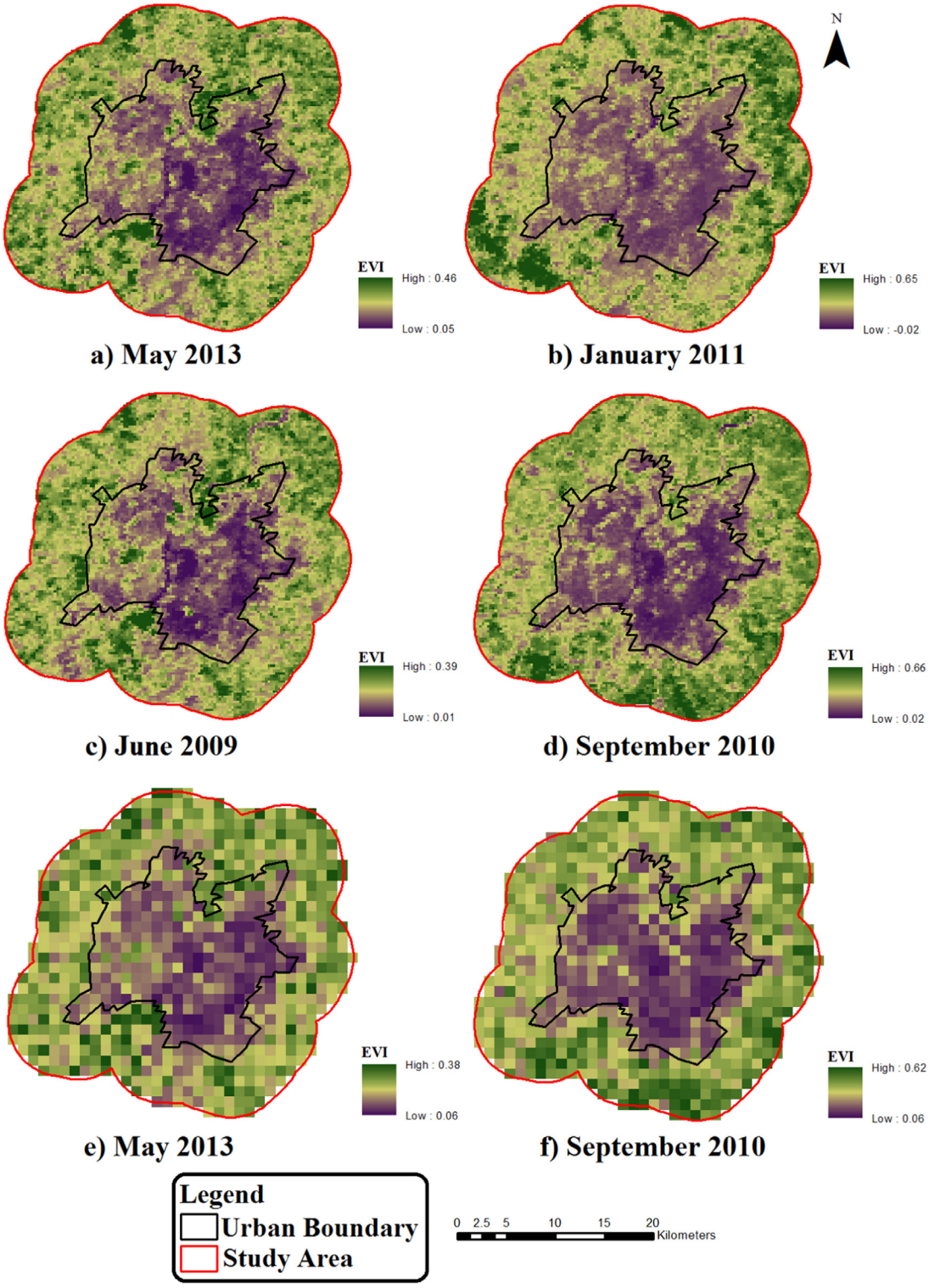

Fig. 7. EVI images of the study area for different seasons.

process. Figs. 6 and 7 show the original NDVI and EVI images (at 231.6 m resolution) and aggregated NDVI and EVI images (at 926.6 m resolution). It is clear from the images that even after aggregation; the general vegetation profile remains the same.

4.3.1. LST relationship with VIs

The scatter plots regarding LST-NDVI relationship for different seasons of a year are shown in Fig. 8. The corresponding LST-EVI scatterplots are also shown in Fig. 9. For the summer season, LST vs. NDVI scatterplots show an irregular and compacted pattern, and most of the NDVI values fall in a narrow range, and a vertical trend can be observed. For monsoon and winter seasons, normally LST vs. NDVI scatterplots show triangular spread. The variation in temperature, for summer and winter images, is higher for low VI values than for high VI values. Vegetation cover is an important parameter which shows the variations in surface temperature of the study area due to the difference in behavior of LU-LC types. The non-vegetated/low-vegetated locations exhibit wide variations in surface temperatures due to the difference in

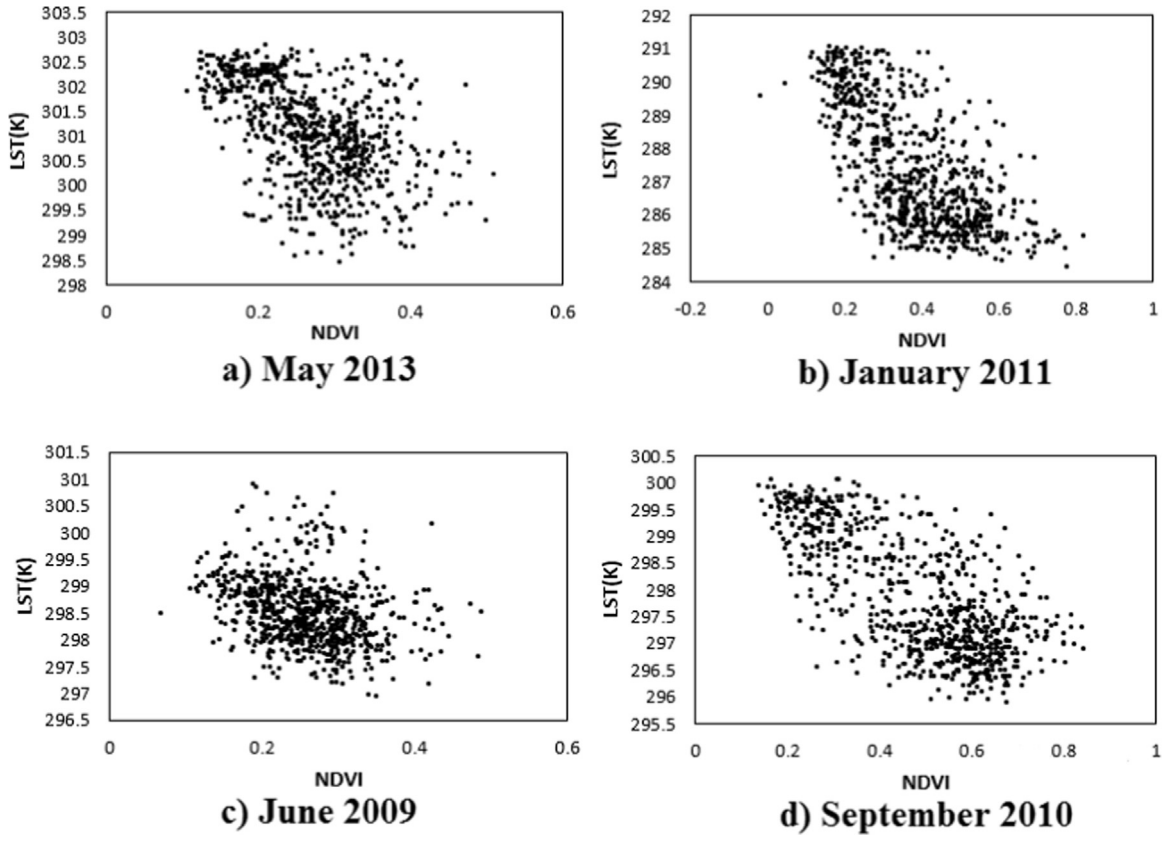

Fig. 8. LST vs. NDVI scatterplots for different seasons.

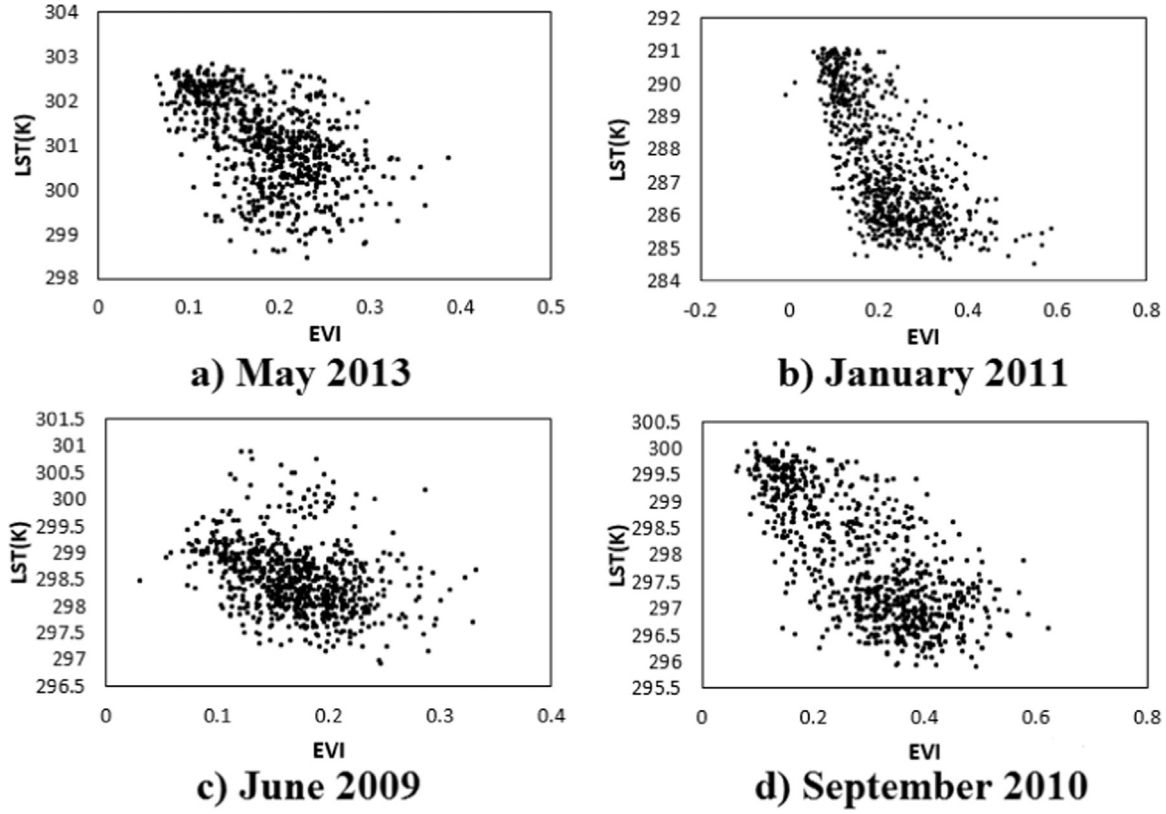

Fig. 9. LST vs. EVI scatterplots for different seasons.

behavior of different LU types, as the LU-LC cover in such locations is highly variable. Results of the research over past few decades have indicated that the surface temperature is determined by both surface soil water content as well as vegetation cover (Carson et al., 1994; Goward et al., 1985; Weng et al., 2004). As discussed above, the vegetation cover over the study area is highly variable. Similarly soil water content also varies depending on various factors such as monsoon rainfall, agricultural practices, etc. Variations in surface temperature are very less in densely vegetated areas. The trend of LST and VIs relationship during different season is different, which clearly indicates that the relationship between LST and VIs is nonlinear and is season dependent. The climate of the study area governs the comparative significance of VI and LST relationship for different seasons. The trend lines of scatter plots show a negative correlation between LST and VIs.

Previous studies (Yuan and Bauer, 2007; Zhang et al., 2009) have found that relationship between LST and NDVI varies with season, which is also validated by the current research. However, they have suggested that NDVI may be used for analysis of SUHI effect during summer and early autumn, whereas the present study for Ahmedabad study area shows that for SUHI studies, VIs may be used during winter

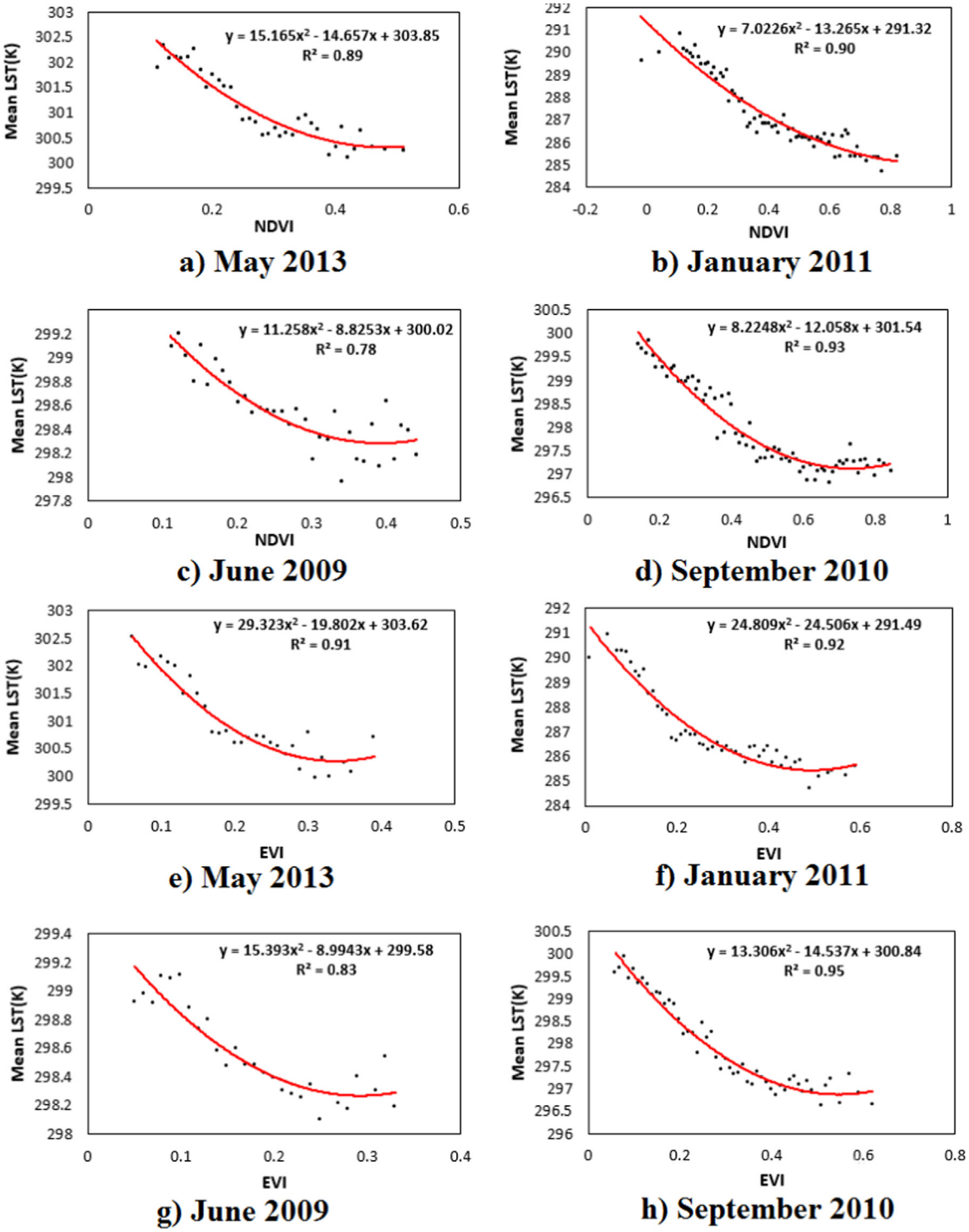

Fig. 10. Mean LST and VI relationship for different seasons.

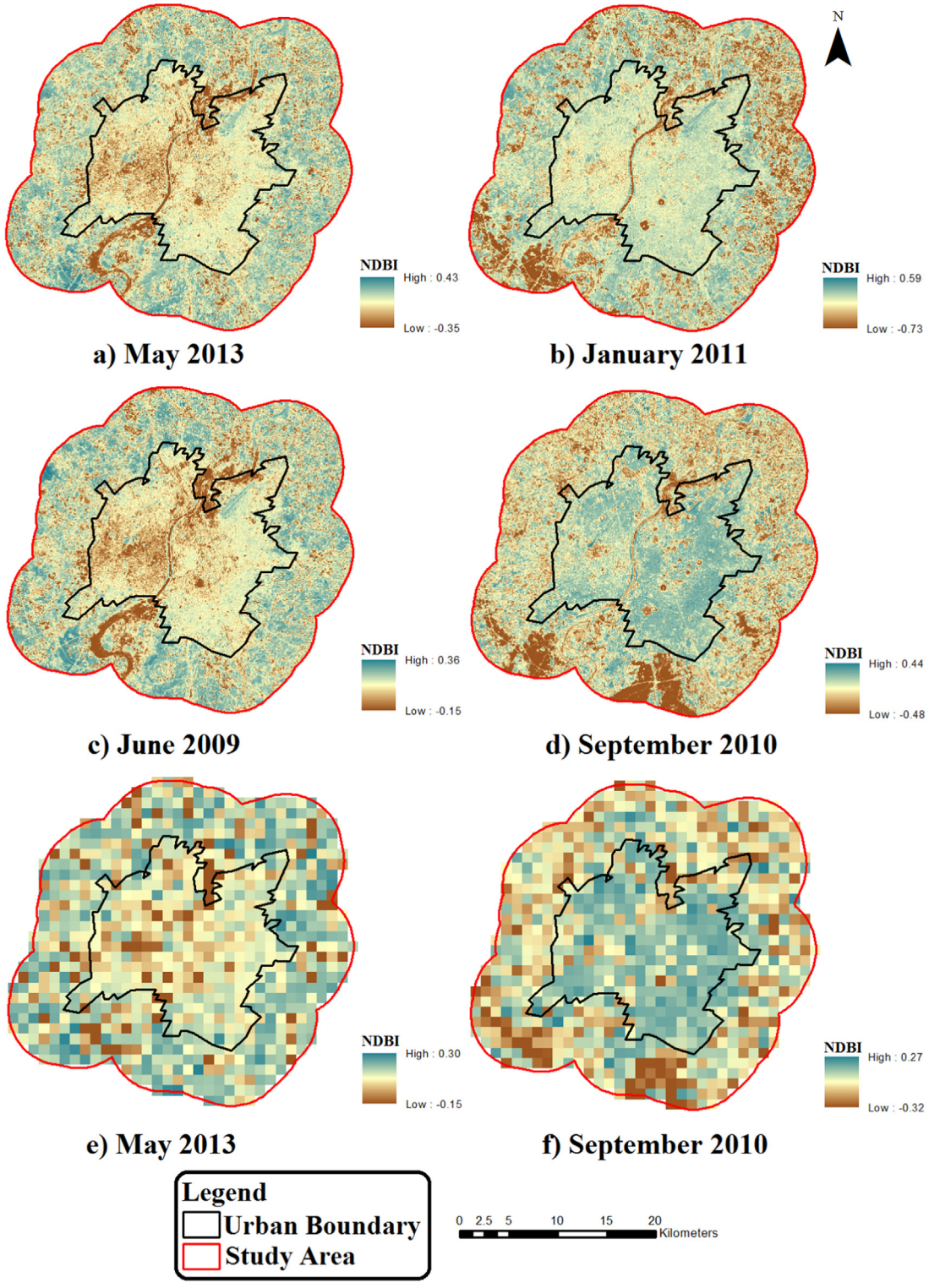

Fig. 11. Landsat NDBI images of the study area for different seasons.

and monsoon seasons also. This difference may be due to different climatic conditions of the studies as the study of Yuan and Bauer (2007) has been carried out for cold climate area of Minnesota whereas the present study area climate is hot and semi-arid. This suggests that the significance of VI and LST relationship for SUHI studies depends on a particular season. However, the general concept that this relationship is good only for the summer season is not entirely true, and the climate of the study area governs the comparative significance of VI and LST relationship for different seasons.

The cooling effect of vegetation on LST of an area is due to the reason that vegetation increases moisture availability and it also has a shadow effect which is due to the shadow of vegetation falling on the nearby surface and thereby modifying the energy interactions which otherwise would have been different in the lack of the vegetation. This is the main reasons of reduction in LST due to the introduction of vegetation at a particular place. It can be expected that as the vegetation density increases, the rate of decrease of LST would reduce beyond a level of vegetation.

4.3.2. Mean LST relationship with VIs

Fig. 10 shows the polynomial relationship between mean LST and VIs for different seasons. The EVI and NDVI range for monsoon and winter season is higher than during summer season. It can be clearly seen that polynomial trend line best represents the mean LST and EVI relationship. Hence second order polynomial relationship between vegetation indices and LST has been proposed and used in the present work.

Fig. 10 shows the relationship between mean LST and VIs for all the three seasons along with the coefficient of correlation (R^2) for the polynomial relationship. Mean LST has been calculated as the average of LST values of pixels having the same index value of vegetation parameters (NDVI and EVI). Most of the previous studies have suggested a linear relationship between NDVI and LST (Tiangco et al., 2008; Yongnian et al., 2010; Yuan and Bauer, 2007; Zhang et al., 2009; Zhangyan et al., 2006). From Fig. 10, it can be observed that the relationship of mean LST with EVI and NDVI is non-linear for all seasons. This may be due to the fact that though the vegetation has an effect on LST yet this effect cannot be same for the entire range of vegetation (or for the corresponding VI values).

The inverse polynomial relationship between mean LST and EVI is more stable (Fig. 10) than the relationship between mean LST and NDVI. However, the relationship tends to break down at highest VI values. Further, it appears that at the highest VI values, there is some increase in the LST values over the LST value corresponding to little lower VI values. The coefficient of correlation during winter and monsoon season shows better values compared to the summer season. R^2 value for LST-NDVI relationship for the winter season of the study period varies from 0.63 to 0.94 with an average value of 0.84. The R^2 value for summer season ranges from 0.52 to 0.90 with a mean value of 0.76. The corresponding average R^2 value for monsoon season is 0.82 with a range of 0.55–0.96. This clearly indicates that for the study area the relationship of NDVI with LST is better for winter season than for summer season. Overall mean R^2 value for LST-NDVI relationship is 0.81. The relationship of mean LST with EVI is almost similar for all the three seasons with an average R^2 value of 0.87, 0.80 and 0.85 for winter, summer and monsoon seasons, respectively with an overall mean R^2 value of 0.84. The relationship of LST with EVI is marginally better than the corresponding relationship with NDVI for the monsoon and winter seasons and significantly better for the summer months. The EVI algorithm utilizes two coefficients for a reduction in atmospheric influences in addition to the use of blue band for correction of the red band for atmospheric aerosol scattering resulting in the better calculation of EVI. Thus, the extent of vegetation is better represented by EVI than by NDVI and hence the better relationship of mean LST with EVI than with NDVI. Therefore, the present study suggests that the MODIS EVI is a better indicator for analysis of SUHI effect when compared with MODIS NDVI.

4.4. Pattern of Normalized Difference Built-up Index (NDBI)

LST is also dependent on urban parameter like NDBI. NDBI is used to automate the process of built-up mapping. It takes use of the unique spectral response of built-up areas and other land covers (Xu, 2006). Wu et al. (2005) have also used NDBI as an urban parameter to extract urban built-up features of Xi'an City in China. NDBI indices are required to characterize the LU-LC types and to explore the quantitative relationships between LU-LC types and SUHI over the study area. The assumption underlying the NDBI method is the spectral reflectance of urban areas in SWIR band exceeding that in NIR band. Because the reflectance of urban areas exhibits little seasonality, this method is not prone to its impact. The disadvantage of NDBI method is unable to distinct urban areas from barren land like sandy regions because both of them have a similar pattern of spectral response in all TM/OLI bands. So especially in summer season, bare soil in rural areas shows higher reflectance in SWIR than NIR resulting in higher values of NDBI in rural areas. However, its performance may be adversely affected indirectly by the presence of other covers whose reflectance is seasonal, such as forest, agricultural fields. NDBI images of different periods, representing different seasons are shown in Fig. 11.

Monsoon NDBI image shows higher values of NDBI representing built-up areas and low values represent vegetation and water. But summer NDBI images show higher values in rural areas than urban areas contrast to monsoon NDBI images. During monsoon and winter seasons, urban area shows higher NDBI values compared to rural areas. Rural areas show higher vegetation density and low bare land density during monsoon season result in higher NDBI values in urban areas. Vegetated areas show very low NDBI values in every season. Water bodies in Ahmedabad city also show very low NDBI values. In the summer season, it has been found out that rural areas show high NDBI values than urban areas because bare soil and sparse vegetation in rural areas show higher spectral reflectance compared to urban areas. Hence from Fig. 11, it is clear that NDBI images show contrast pattern during different seasons mainly due to the ambiguity in LU-LC changes. So NDBI cannot be used as an urban parameter for the extraction of built-up areas especially in semi-arid regions where bare land density is higher.

The values of NDBI have been calculated at the Landsat TM resolution of 30 m and the aggregated resolution of 926.6 m. The overall absolute maximum and minimum NDBI values of the study area are 0.64 and − 0.97, respectively. The overall average NDBI value over the study area is 0.17. Monsoon and winter season exhibit higher NDBI range than the summer season. Fig. 11 shows the original NDBI image (at 30 m resolution) and aggregated NDBI image (at 926.6 m resolution), respectively. It is evident from the images that even after aggregation; the general NDBI profile remains the same.

4.4.1. LST relationship with NDBI

The NDBI has been developed for the identification of urban and built-up areas (Zha et al., 2003). The scatter plots regarding LST-NDBI relationship for different seasons are shown in Fig. 12. LST vs. NDBI scatterplots show an irregular, and compacted pattern and a horizontal trend can be observed for all seasons. For monsoon and winter seasons, the trend line of scatterplots shows positive relation in between LST and NDBI. But for the summer season, the trend lines of scatterplots show a linear or negative correlation in between LST and NDBI. Generally, bare soil in rural areas shows high spectral reflectance in SWIR band compared to urban built-up areas. Drier or sparse vegetation can also even show higher reflectance in SWIR wavelength range than in NIR range (Gao, 1996), resulting in positive NDBI values in NDBI images for drier vegetation. So in the summer season, the soil in rural areas shows higher NDBI values as compared to urban areas. For winter and monsoon season, urban areas show higher NDBI values compared to rural areas. So the scatterplots show positive trend line during monsoon and winter season. The trend of LST-NDBI relationship during different season is different, which clearly indicates that the relationship between LST and NDBI is linear and is season dependent. NDBI performance may be adversely affected indirectly by the presence of other covers whose reflectance is seasonal, such as vegetation. Higher vegetated areas in rural areas show very low values of NDBI. So in monsoon season, rural areas show very low NDBI values.

In some conditions, water with high suspended matter concentration (SMC) can also reflect SWIR stronger than NIR because the reflectance peak can shift to longer wavelength regions when the suspended matter content upsurges. Therefore, the drier or sparse vegetation and water with high SMC will show positive NDBI values and present as noise in a NDBI image. The contrast of the NDBI image is not so worthy to extract urban features because many pixels having vegetation and water features show positive NDBI values with medium gray tones and exist as noise mixed with built-up land features (Xu, 2007). These suggest that the urban landscapes could not be extracted merely based on a NDBI image, and NDBI cannot be used as a good

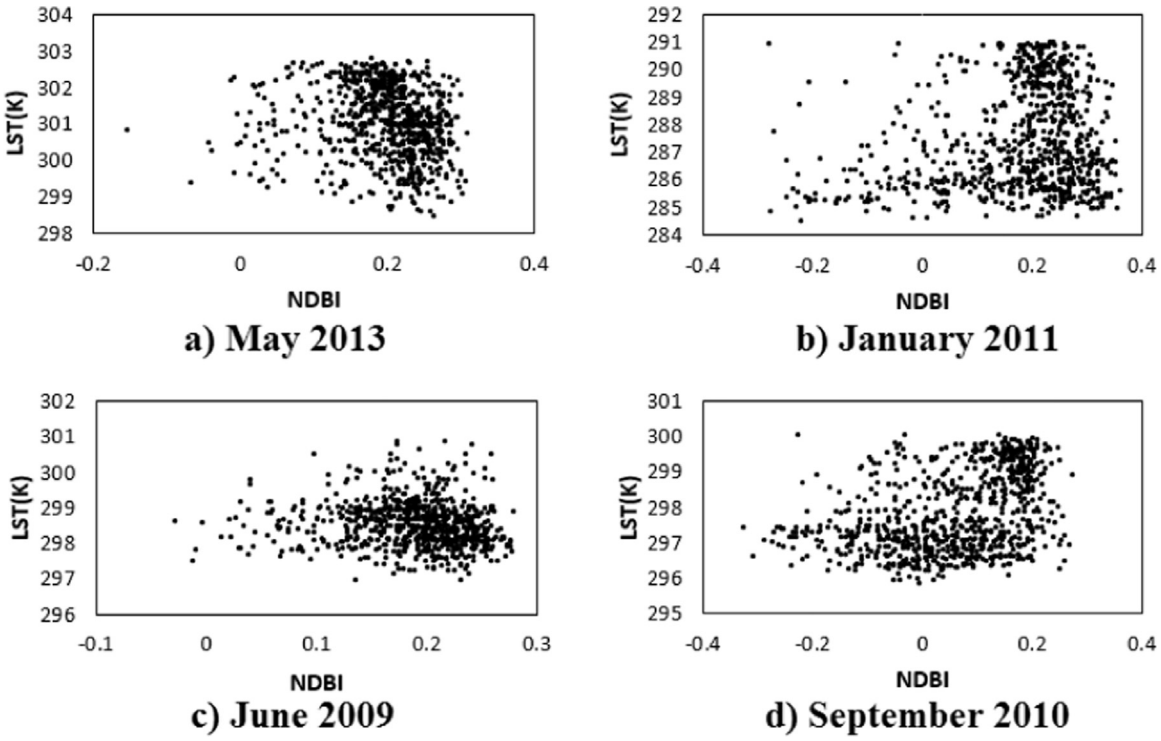

Fig. 12. LST vs. NDBI scatterplots for different seasons.

urban parameter for SUHI studies.

Fig. 13 shows the relationship between mean LST and NDBI for all the seasons along with the coefficient of correlation (R^2). A negative correlation has been observed between LST and NDBI during the summer season with less coefficient of correlation. The R^2 value for summer season varies from 0.02 to 0.15 with an average value of 0.08. A positive correlation has been observed between LST and NDBI during monsoon and winter season with moderate R^2 values. The corresponding average R^2 value for monsoon season is 0.63 with a range of 0.52–0.67. The corresponding average R^2 value for the winter season is 0.34 with a range of 0.25–0.43. This clearly indicates that for the study area, the relationship of NDBI with LST is comparatively good for winter and monsoon season with positive correlation than for summer season. Overall mean R^2 value for LST-NDBI relationship has been found out to be 0.35. It has been observed that the graph between mean LST and NDBI shows rising trend with less R^2 values, especially

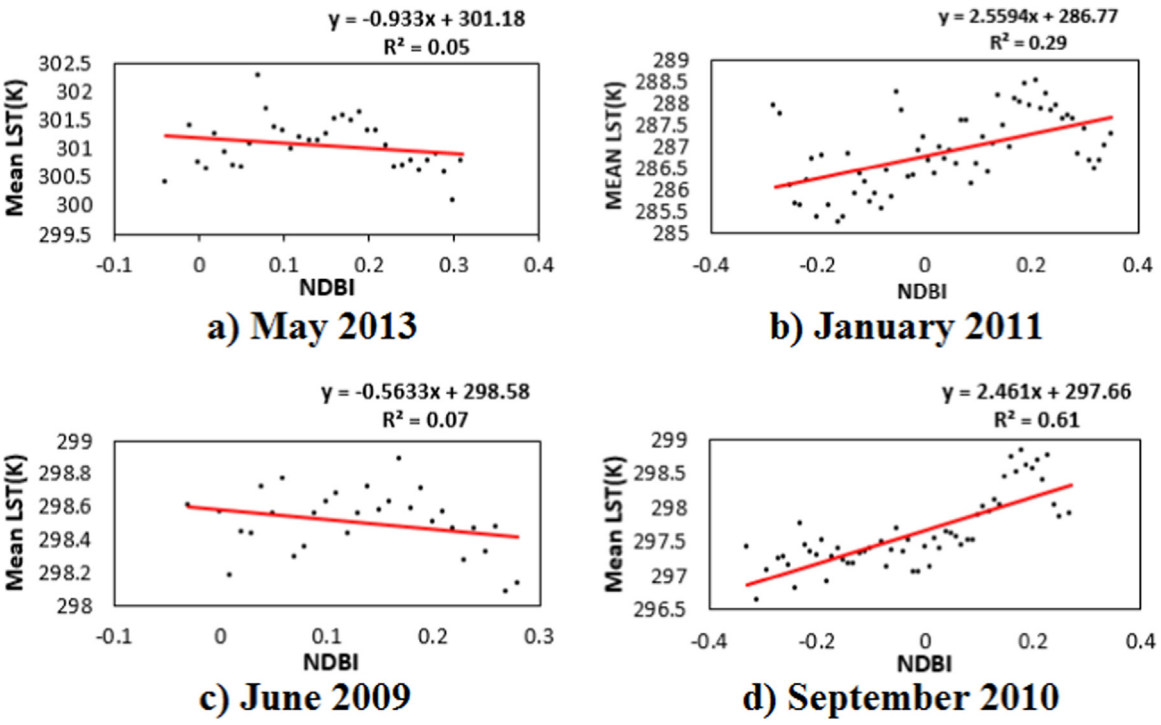

Fig. 13. Mean LST and NDBI relationship for different seasons.

during monsoon and winter season. In winter and monsoon season, the graph shows a positive correlation between LST and NDBI. But in the summer season, the graph shows a negative correlation between LST and NDBI with very low R^2 values due to the effect of lighter soil in rural areas on NDBI. The coefficient of correlation during monsoon season has been found to be higher than compared to summer and winter season. The relationship between NDBI and LST shows very weak contrast relationship during different seasons, and hence NDBI cannot be used as an urban parameter for SUHI studies in semi-arid regions where bare land density higher as compared to vegetation density.

4.5. Pattern of Percent Impervious Surface Area (%ISA)

%ISA has emerged as a key factor to explain and predict the degree of impact severity on LST. Imperviousness gives an objective measurement of the areal extent and intensity of urban development. The linear spectral unmixing method has been used to extract impervious surfaces from the study area using ENVI software. The resulting classification gives a continuous range of %ISA from 0% to 100%. %ISA is a season independent parameter representing urbanization. In order to analyze the spatial pattern of impervious surfaces of the study area, % ISA images of the study area for different periods are shown in Fig. 14. Urban areas have higher %ISA values and appear green while highly vegetated areas appear brown in the figure. During the summer season, most of the rural area shows light brown spots of low %ISA values which represent bare soil while dark brown spots represent dense vegetation. Very limited green spots have been observed in the rural area especially in the western parts of the study area, which indicate low imperviousness in the rural area. Most of the green spots representing higher %ISA values are observed within the urban boundary, especially central and eastern parts of the city. The %ISA pattern in the urban area has been found to be almost same during different seasons from 2009 to 2013 with a similar trend. Rural areas show changes in %ISA pattern during different seasons due to the LU-LC changes which are almost insignificant, because of vegetation and bare land exhibit very low % ISA values which are almost equal to zero.

Urban areas show higher values of %ISA compared to rural areas due to the presence of impervious surfaces like buildings, pavements, parking lots, etc. Agricultural land and vegetated areas in rural areas show zero %ISA. Bare soil in rural areas shows very low values of %ISA compared to urban areas.

The values of %ISA have been estimated at the Landsat TM/OLI resolution of 30 m and at the aggregated resolution of 926.6 m. The overall absolute maximum and minimum %ISA values of the study area are 0 and 100, respectively. The overall average of the %ISA of the study area varies from 25.26% to 36.92%. Fig. 14 shows the original % ISA image (at 30 m resolution) and aggregated %ISA image (at 926.6 m resolution). From the images, it is obvious that the general %ISA profile remains the same even after aggregation.

4.5.1. LST relationship with %ISA

The scatter plots of LST-%ISA relationship for different years are shown in Fig. 15. The relationship between %ISA and LST is similar for all three seasons with a consistent rising trend (Fig. 15). Though high variation can be observed in the scatter plots showing a weak trend for low %ISA values, but the trend is strong for high %ISA values. Normally %ISA values are very less in rural areas compared to urban areas due to the lack of impervious surfaces like roads, built-up areas, etc. which results in weak trend and also the presence of bare land, vegetation cover and agricultural field shows very low %ISA values in rural areas which lead to low LST. The weak trend may be due to the fact that for low %ISA values, the effect of urbanization is insignificant and hence LST variations are governed by the combined effect of several other parameters such as vegetation cover and its disposition, type and extent of surface imperviousness, the condition of nearby pixels, etc. The improved trend for higher %ISA values indicates that for an urbanized area, %ISA, compared to other parameters, has more effect on LST. Similar trend for different seasons indicates that unlike VIs the relationship of %ISA with LST is independent of season.

Yuan and Bauer (2007) have documented a strong linear relationship between the amount of impervious surface area and LST or the SUHI effect in the field of urban climate which is also validated by the present study. Vegetation is also dependent on the extent of urbanization, and vegetation density normally decreases with increase in urbanization. %ISA is an indicator of urbanization which increases with city growth. It also takes into account, to some extent, the effect of anthropogenic heat produced due to various human activities taking place in urban areas such as industries, heat produced due to air-conditioning, vehicular traffic, etc. Hence the analysis of SUHI effect using %ISA not only considers the impervious surfaces but it also accommodates, to some extent, the influence of anthropogenic heat, which is one of the main reasons to the SUHI effect. This explains the constant rising pattern between LST and %ISA.

Fig. 16 shows the relationship between mean LST and %ISA for all seasons. Most of the previous studies have suggested a linear relationship between %ISA and LST (Yuan and Bauer, 2007; Zhang et al., 2009). Second order polynomial nonlinear relationship of LST with % ISA has been used in the study, and polynomial relationships are marginally better than the linear relationship. Normally the graph correlating mean LST and %ISA shows rising trend in all seasons along with the coefficient of correlation (R^2). The R^2 value for summer season varies from 0.60 to 0.82 with an average value of 0.73. The corresponding average R^2 value for monsoon season is 0.78 with a range of 0.62–0.85. The corresponding average R^2 value for the winter season is 0.82 with a range of 0.65–0.87. This clearly indicates that for the study area the relationship of %ISA with LST is better for winter season than for summer season. Overall mean R^2 value for LST-%ISA relationship is 0.77. The coefficient of correlation during winter season shows higher values compared to monsoon and summer season. So for the study area, the relationship between mean LST and %ISA is better during winter season than the summer season. A positive correlation has been observed between LST and %ISA, and this relationship has been found to be consistently similar during all the three seasons. This indicates that the relationship between LST and %ISA is independent of season. Similar trend for different seasons indicates that unlike VIs the relationship of %ISA with LST is independent of season. Though vegetation is significantly dependent on the extent of urbanization and it generally decreases with increase in urbanization, yet in the study area, it is also dependent on rainfall during monsoon season. %ISA has been considered to include the indirect effect on the rise in temperature due to anthropogenic heat in addition to the direct effect due to the imperviousness of urban surfaces.

The overall analysis of the relationship of LST with different parameters indicates that the relationship of %ISA with LST is better than the corresponding relationship of LST with NDBI. The association between LST and NDBI has limitations with regards to the season and the relationship between mean LST and NDBI; though has almost different trend for different seasons, it is inferior to corresponding mean LST and %ISA relationship. %ISA can be used to reflect the seasonal and temporal fluctuations in similar polynomial patterns, but with different governing relationship equations of better coefficient of determination. Hence, %ISA is a better indicator for the analysis of SUHI effect, with no dependence on the season.

4.6. Road network and road density maps

Fig. 17 shows the final road network map of the study area. The total length of roads in the study area is around 7085 km. The effect of urbanization can be clearly understood from the road network map, and it can be seen that the urban area has extensive road network. The length of roads in rural and semi-urban areas is very less as compared to

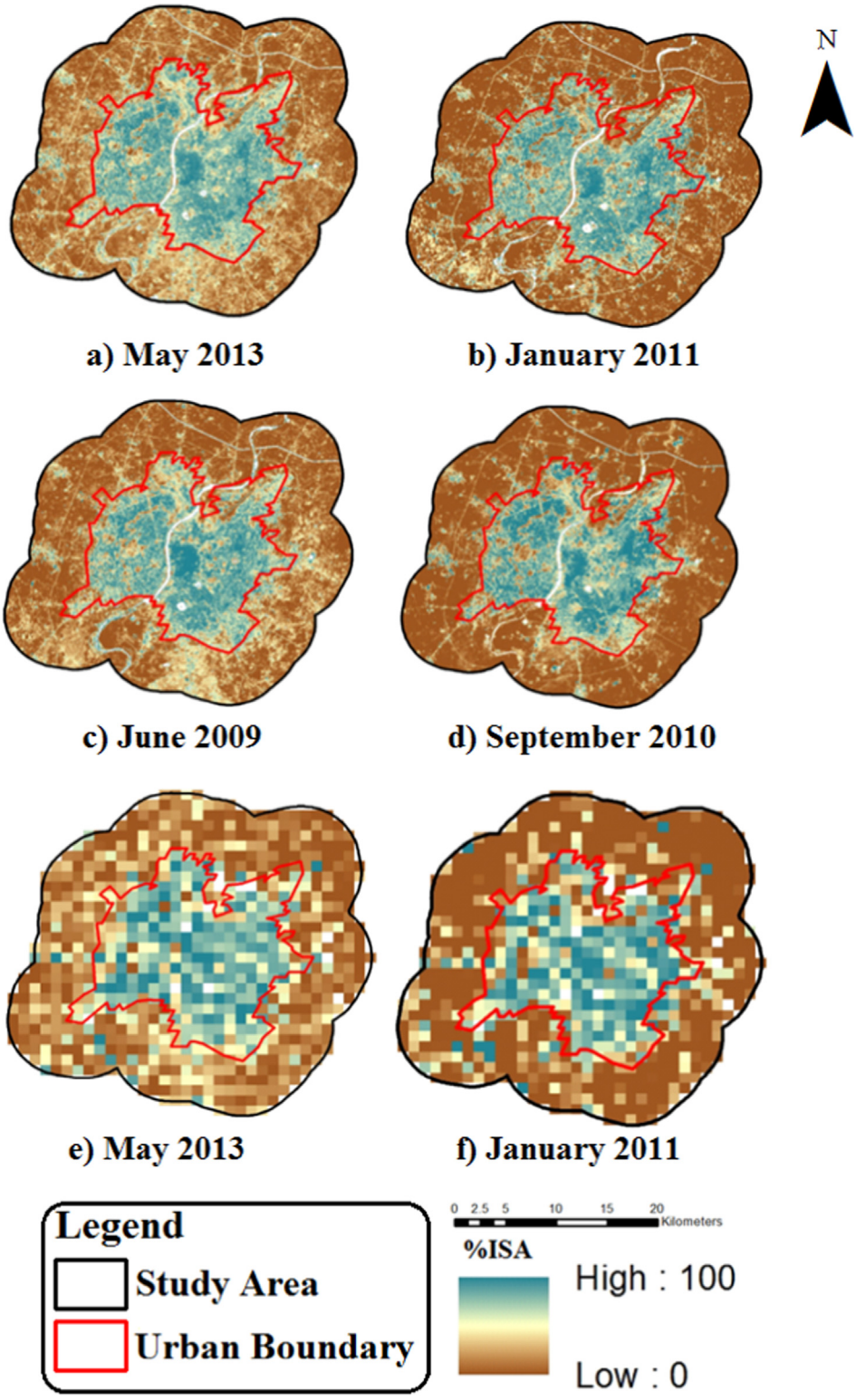

Fig. 14. %ISA images of the study area for different seasons.

that in the urban area. Some signs of development in the form of an increase in road network can also be seen outside the West and North-Western part of the urban boundary. The length of roads is minimum in the Southern zone as most of the area of this zone comprises of agricultural fields. Within the urban area also some patches of lower road network can be seen corresponding to central parts of the city due to water bodies like Sabarmati river. Kankaria and Chandola lakes in Southern part of the city and parks in different parts of the city resulting lower road network in some parts of the urban area.

The road network map has been used to calculate RD for every pixel of the study area. The nighttime MODIS LST product used for the present study is at 926.6 m resolution. Hence the radius, for calculating RD by line density tool, has been taken as 655 m, which is the radius of a circle inscribing one complete LST pixel. The cooling/heating of a pixel depends not only on the incident solar radiation and surface properties, but it also depends on conditions of the nearby pixels. The area of the

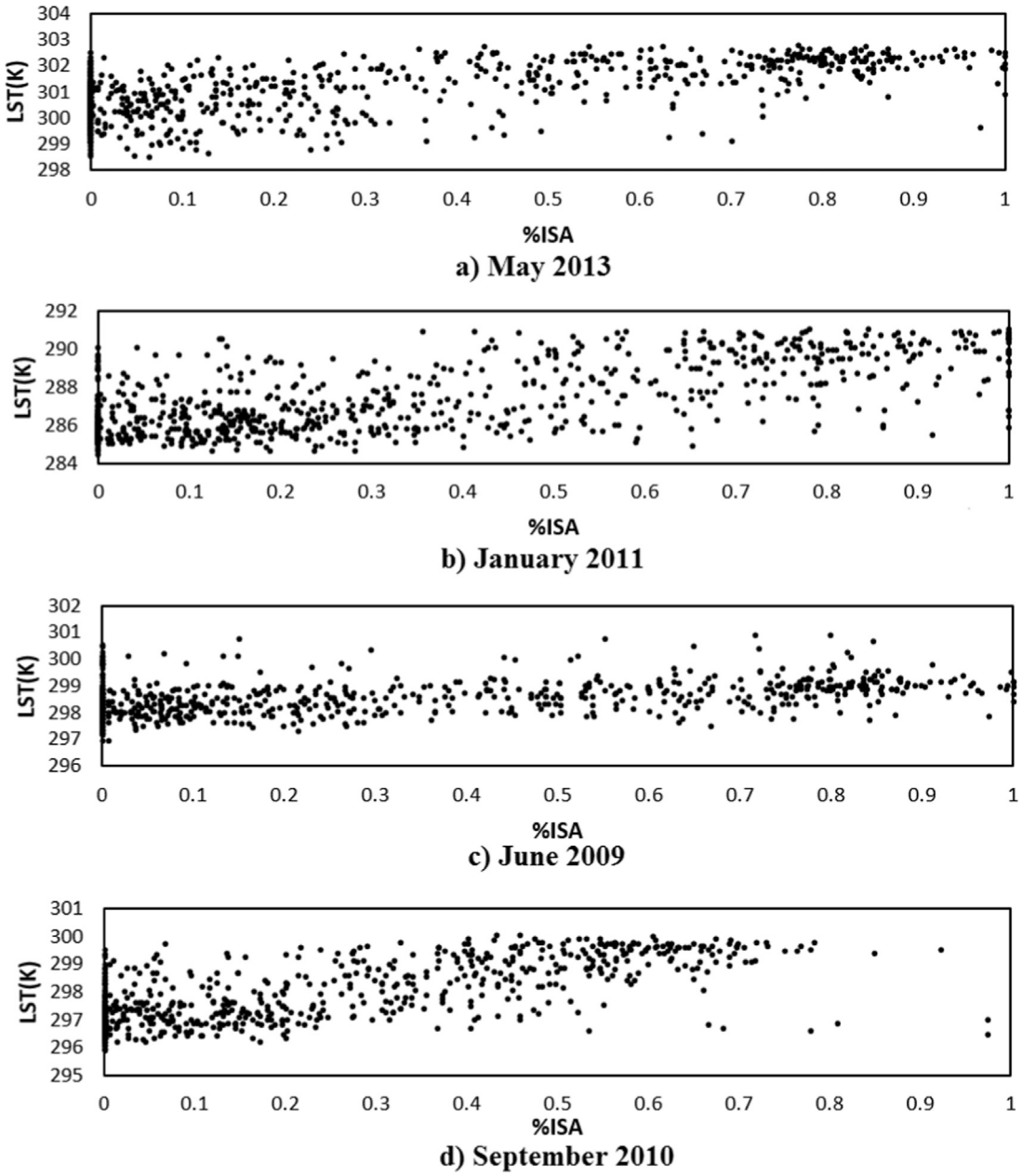

Fig. 15. LST vs. %ISA scatterplots for different seasons.

circle considered for calculating RD of a pixel is 57% more than the area of the corresponding pixel, and calculating RD by this method takes into account some effect of nearby pixels also. The values of RD vary from zero to 39.44 km per square km. Fig. 17 shows the RD map of the study area. RD of the suburban area is much lower than the RD of the urban area.

Fig. 17 shows RD map of Ahmedabad study area having higher RD in urban areas and lower in rural and semi-urban areas. RD of Ahmedabad study area ranges from 0 to 39.44 km/sq. km with a mean RD of 10.27 km/sq. km. RD of Ahmedabad urban area ranges from 2.09 to 39.44 km/sq. km with a mean RD of 18.64 km/sq. km. RD of Ahmedabad rural area ranges from 0 to 32.68 km/sq. km with a mean RD of 6.27 km/sq. km, i.e., mean RD of the rural area is only about 30% of the mean RD of the urban area.

4.6.1. LST relationship with RD

The relationship between RD and LST is similar for all three seasons with a consistent rising trend (Fig. 18). Though high variation can be observed in the scatter plots showing a weak trend for low RD values, but the trend is strong for high RD values. The weak trend may be due to the fact that for low RD values, urbanization does not have a significant effect and hence LST variations are governed by the combined effect of several other parameters such as vegetation cover and its disposition, type, and extent of surface imperviousness, condition of nearby pixels, etc. The improved trend for higher RD values indicates that for an urbanized area, RD, compared to other parameters, has more effect on LST. Similar trend for different seasons indicates that unlike VIs the relationship of RD with LST is independent of season. Though vegetation is greatly dependent on the extent of urbanization and the vegetation density typically decreases with increase in urbanization, yet in the study area, it is also dependent on rainfall during monsoon season. RD is also an indicator of urbanization which increases with the growth of the city. It also takes into account, to some extent, the effect of anthropogenic heat generated due to various human activities taking place in urban areas such as industries, heat due to air-conditioning, vehicular traffic, etc. Hence the analysis of SUHI effect using RD not

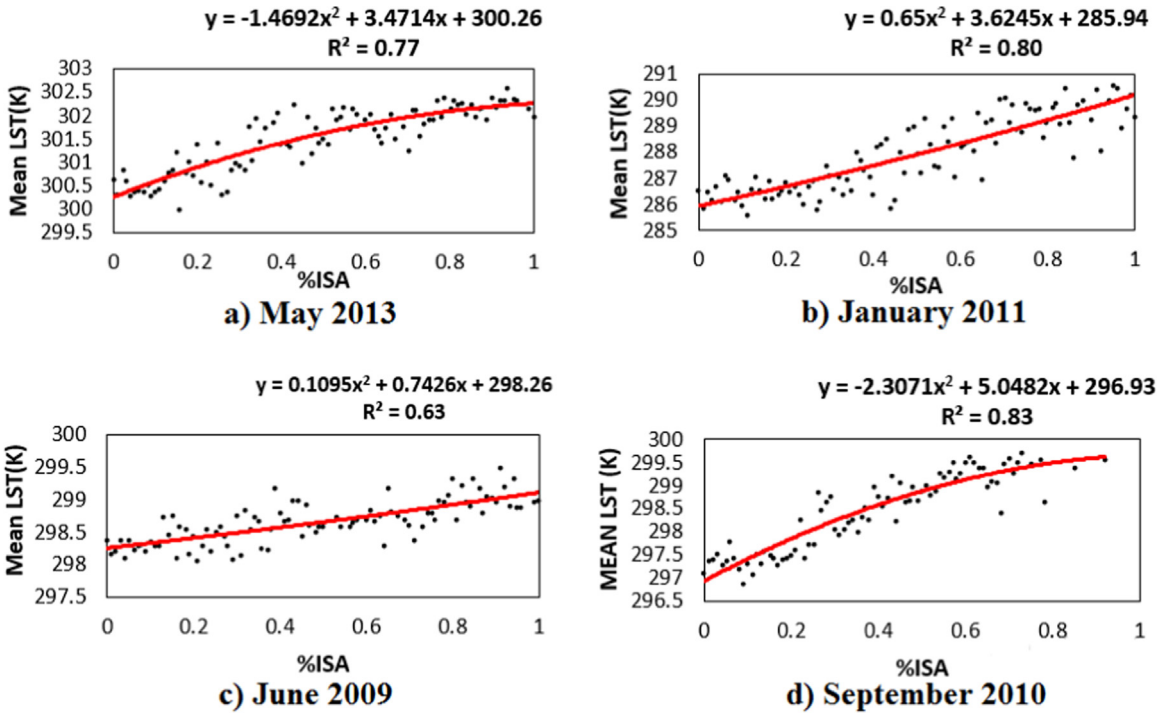

Fig. 16. Mean LST and %ISA relationship for different seasons.

only considers the impervious surfaces but it also includes, to some extent, the influence of anthropogenic heat, which is one of the primary contributors to the SUHI effect. This explains the constant rising pattern between LST and RD.

The relationship between mean LST and RD is very strong for all the three seasons (Fig. 19). In this case also, the rate of increase in mean LST is higher for low values of RD and drops significantly for higher values of RD. Hence polynomial relationship of second order is proposed for the relationship between mean LST and RD also. Though the relationship of LST with RD has weak trend for the low RD values (Fig. 19), but the use of mean LST normalizes the local effects of other parameters over particular pixels and the relationship of mean LST with RD is strong for different seasons. Strong mean LST and RD relationship can be observed for the winter season with an average R^2 value of 0.84. The average R^2 value for the relationship between LST and RD during monsoon season is 0.81 and maximum and minimum values are 0.89 and 0.78, respectively. The R^2 value is low for some periods of monsoon season of one year, but during the same period of other years, this value is not that low and even higher than 0.85 during some years. This indicates that the low R^2 value, during some observations, is due to some local effect during that period only. During the summer season, the average R^2 value is 0.75, and even the lowest value is 0.65 which is reasonably good. During most of the periods of the summer season, the R^2 value is more than 0.75, thus indicating a good relationship between mean LST and RD during summer season also. Overall mean R^2 value for mean LST-RD relationship is 0.80. These high R^2 values for all periods/seasons of different years indicate that LST variations can be accounted for very well by RD for all the seasons and RD can be used as

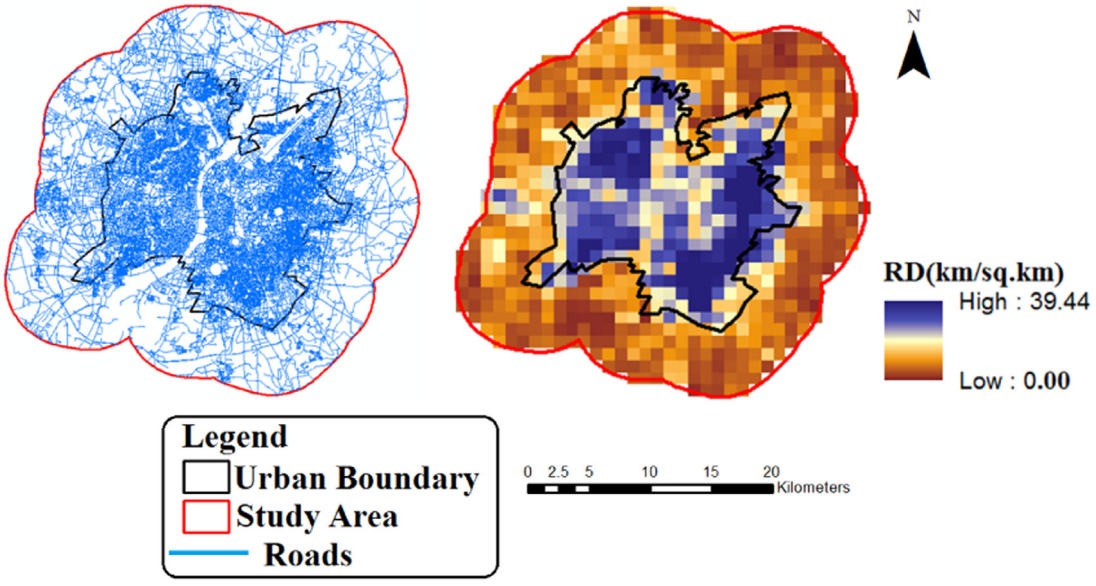

Fig. 17. Road network and Road Density map of the study area.

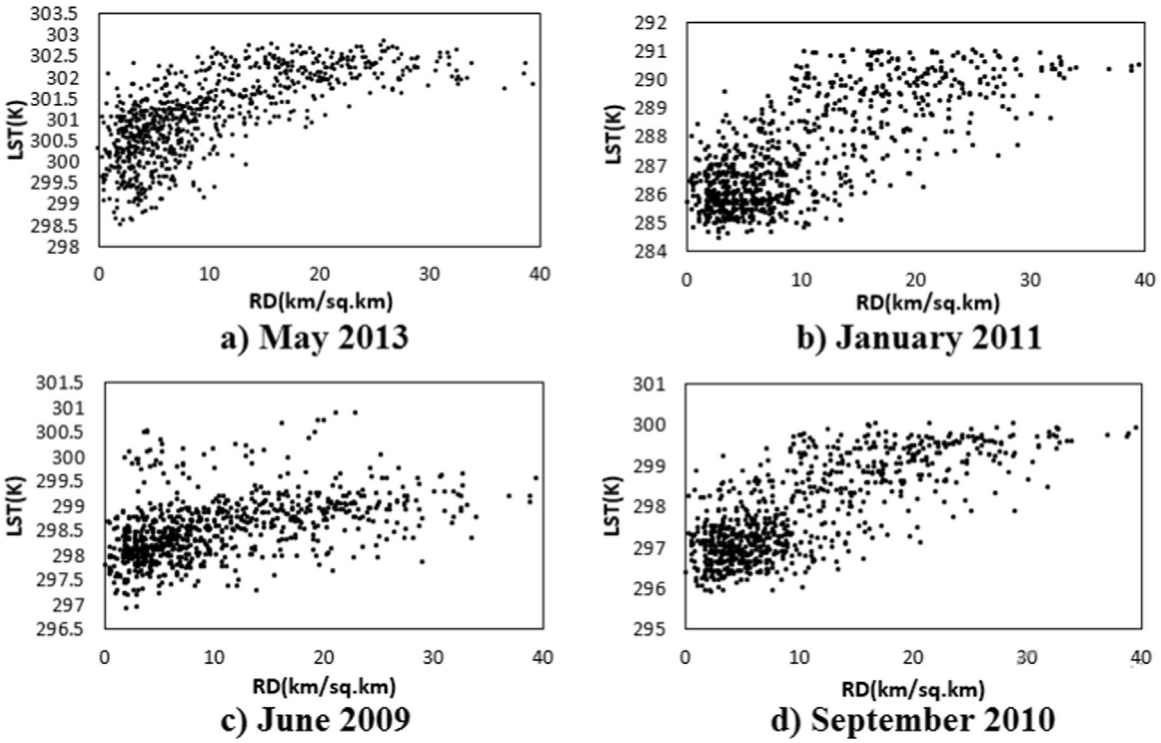

Fig. 18. LST and RD relationship for different seasons.

a parameter, across all seasons, for SUHI studies.

5. Conclusion

In the present study, LST, NDVI, EVI, %ISA, RD, and NDBI have been derived using Landsat TM, OLI and MODIS sensor data and the relationships of LST with vegetation and urbanization parameters have been investigated in the Ahmedabad study area. It is noted that most of the hot pixels are located at the central part of the Ahmedabad city, and the rural areas show less LST compared to urban areas because of the presence of dense vegetation. The areas with built-up areas and human activities show high LST compared to green vegetative areas. So built-up areas including residential, commercial and industrial mainly account for SUHI effect over Ahmedabad study area. Urban sprawling contributes the major changes in the LST which leads to the variations in SUHI over Ahmedabad study area. Eight-day nighttime LST has been

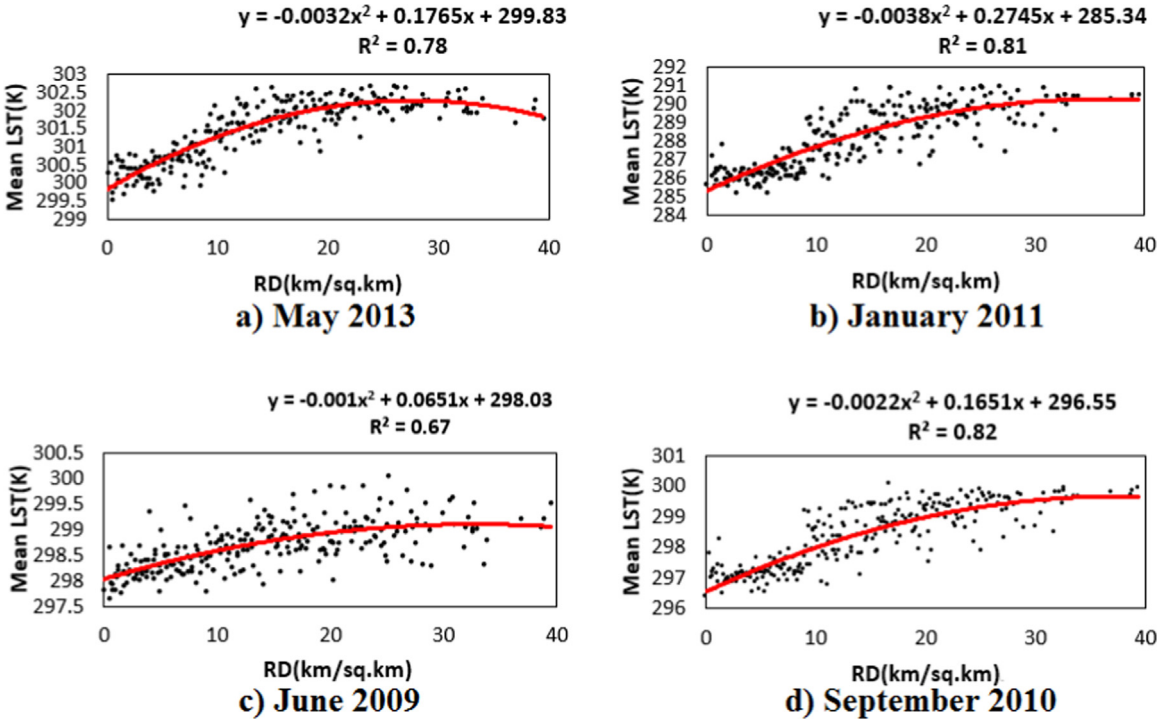

Fig. 19. Mean LST and RD relationship for different seasons.

utilized in the present study, for the analysis of UHI effect over Ahmedabad city in India, which has been undertaken for summer, monsoon and winter seasons. Significant SUHI has been observed in the study area from the analysis of five years LST data from 2009 to 2013. The central part of Ahmedabad urban area that comprises the CBD of Ahmedabad city encounters maximum LST due to predominantly built-up and paved areas in the CBD. Average $SUHI_{index}$ of 5 pixels falling in CBD is more than 0.90 which indicates that high LST normally occurs on these pixels and they can be considered as hot spots (HS) with a maximum average $SUHI_{index}$ of 0.93. The HS act as the center of SUHI of Ahmedabad city and other high-temperature pixels are located around these pixels. Significant variations in SUHI intensity over the entire study area have been observed. Average SUHI intensity of different seasons varies from 4.68 K to 7.40 K. Overall average SUHI intensity of the study area during monsoon, summer and winter seasons is 5.38 K, 6.06 K, and 7.07 K, respectively. Overall average SUHI intensity of the study area for all seasons is 6.17 K. Central part of the Ahmedabad city is extremely hot compared to other parts of the city because of a large number of roads, complex infrastructure, and high peak buildings. In the case of Ahmedabad study area, minimum LSTs are observed over the area at the boundary of the study area, especially on the South Western side.

In the present study, it has been observed that there is a negative relationship between LST and NDVI or EVI during the entire seasons. Mean LST vs. VIs graph shows better relationship during winter season compared to the summer season. EVI better represents the extent of green vegetation than by NDVI and hence mean LST with EVI shows better relationship than NDVI. Hence EVI is a better indicator than NDVI for SUHI studies. In the present study, urban parameters NDBI, % ISA, and RD which represent the extent of urbanization has been used for the SUHI analysis. A positive relationship has been observed between LST and %ISA. The relationship between LST and %ISA is almost same throughout the entire season for the study area with a consistent rising trend. Though high variation can be observed in the scatter plots showing a weak trend for low %ISA values, but the trend is strong for high %ISA values. In the mean LST vs. %ISA relationship, it has been observed that the coefficient of correlation of winter season has been found to be higher compared to monsoon and summer seasons. A positive relationship has been found between LST and RD, and this relationship has been found to be consistently similar during all the three seasons. This indicates that the relationship between LST and RD is independent of season. RD has been considered to include the indirect effect on the rise in temperature due to anthropogenic heat in addition to the direct effect due to the imperviousness of urban surfaces. High R^2 values for the relationship between mean LST and RD for different periods and different seasons of the entire study period indicate that the relationship between LST and RD is not only independent of the season, but the variations in LST can be accounted very well by RD.

A positive relationship has been found between LST and NDBI especially for monsoon season. The trend of LST and NDBI relationship during different season is different, which clearly indicates that the relationship between LST and NDBI is linear and is season dependent. In the mean LST vs. NDBI relationship, it has been observed that the coefficient of correlation of monsoon season has been found to be higher compared to summer and winter seasons. Normally NDBI shows better values during monsoon season, so LST-NDBI relationship is much better during monsoon months as compared to winter and summer months. Normally bare soil in rural areas shows high spectral reflectance in SWIR band compared to urban built-up areas. Drier vegetation can also even show higher reflectance in SWIR wavelength range than in NIR range, resulting in positive NDBI values in NDBI imagery for these plants. Hence NDBI cannot be used as a good indicator for SUHI studies where bare land, includes soil and drier vegetation, is predominant in rural areas, especially for the summer season. So for the summer months, the trend lines of scatterplots show a linear or negative correlation in between LST and NDBI. Hence %ISA and RD have been found to be better urbanization parameters for SUHI studies compared to NDBI.

Overall analysis of the relationship of LST with all the different parameters indicates that a very complex relationship exists between them. Though NDVI, EVI, %ISA, NDBI, and RD are independent parameters and uniquely affect the LST, but they are influenced, to some extent, by each other also. Most of the previous studies have analyzed the LST variations as an effect of single parameter individually and have not considered the simultaneous effect of several parameters. It may, therefore, be important to determine the combined effect of all these parameters on LST. Considering the seasonal and temporal variations in the LST, $SUHI_{index}$ has been used for the study of the simultaneous effect of several parameters on LST.

Acknowledgement

This work was supported by the Department of Science and Technology (DST) Delhi, Government of India. The authors wish to thank the anonymous reviewers for their valuable comments, which helped to improve this paper. The authors wish to thank the Land Processes Distributed Active Archive Center (LP DAAC), located at the U.S. Geological Survey (USGS) Earth Resources Observation and Science (EROS) Center (lpdaac.usgs.gov) for making available the satellite data.

References

Aguiar, R., Oliveira, M., Gonccedilalves, H., 2002. Climate change impacts on the thermal performance of Portuguese buildings. Results of the SIAM study. Build. Serv. Eng. Res. Technol. 23 (4), 223–231.
Alshaikh, A.Y., 2015. Space applications for drought assessment in Wadi-Dama (West Tabouk), KSA. Egypt. J. Remote Sens. Space Sci. 18, 543–553.
Aniello, C., Morgan, K., Busbey, A., Newland, L., 1995. Mapping micro-urban heat Islands using Landsat TM and a GIS. Comput. Geosci. 21 (8), 965–969.
Borbora, J., Das, A.K., 2014. Summertime Urban Heat Island study for Guwahati City, India. Sustain. Cities Soc. 11, 61–66.
Carson, T.N., Gillies, R.R., Perry, E.M., 1994. A method to make use of thermal infrared temperature and NDVI measurements to infer surface soil water content and fractional vegetation cover. Remote Sens. Rev. 9, 161–173.
Chen, X.-L., Zhao, H.-M., Li, P.-X., Yin, Z.-Y., 2006. Remote sensing image-based analysis of the relationship between urban heat island and land use/cover changes. Remote Sens. Environ. 104 (2), 133–146.
Cheval, S., Dumitrescu, A., 2009. The July urban heat island of Bucharest as derived from MODIS images. Theor. Appl. Climatol. 96, 145–153.
Civco, D.L., Hurd, J.D., Wilson, E.H., Arnold, C.L., Prisloe Jr., M.P., 2002. Quantifying and describing urbanizing landscapes in the northeast United States. Photogramm. Eng. Remote Sens. 68 (10), 1083–1090.
Clinton, N., Gong, P., 2013. MODIS detected surface urban heat islands and sinks: global locations and controls. Remote Sens. Environ. 134, 294–304.
Deng, C., Wu, C., 2013. Examining the impacts of urban biophysical compositions on surface urban heat island: a spectral unmixing and thermal mixing approach. Remote Sens. Environ. 131, 262–274.
Dezső, Zs, Bartholy, J., Pongrácz, R., 2005. Satellite based analysis of the urban heat island effect. Időjárás 109, 217–232.
Dousset, B., Gourmelon, F., 2003. Satellite multi-sensor data analysis of urban surface temperatures and land cover. ISPRS J. Photogramm. Remote Sens. 58 (1–2), 43–54.
Gallo, K.P., McNab, A.L., Karl, T.R., Brown, J.F., Hood, J.J., Tarpley, J.D., 1993. The use of NOAA AVHRR data for assessment of the urban heat-island effect. J. Appl. Meteorol. 32 (5), 899–908.
Gallo, K.P., Easterling, D.R., Peterson, T.C., 1996. The influence of land use/land cover on climatological values of the diurnal temperature range. J. Clim. 9, 2941–2944.
Gao, B.C., 1996. NDWI–A normalized difference water index for remote sensing of vegetation liquid water from space. Remote Sens. Environ. 58 (3), 257–266.
Gillies, R., Kustas, W., Humes, K., 1997. A verification of the 'triangle' method for obtaining surface soil water content and energy fluxes from remote measurements of the Normalized Difference Vegetation Index (NDVI) and surface. Int. J. Remote Sens. 18 (15), 3145–3166.
Goward, S.N., Cruickshank, G.D., Hope, A.S., 1985. Observed relation between thermal emission and reflected spectral radiance of a complex vegetated landscape. Remote Sens. Environ. 18, 137–146.
Guo, G., Wu, Z., Xiao, R., Chen, Y., Liu, X., Zhang, X., 2015. Impacts of urban biophysical composition on land surface temperature in urban heat island clusters. Landsc. Urban Plan. 135, 1–10.
Holme, A.Mc.R., Burnside, D.G., Mitchell, A.A., 1987. The development of a system for monitoring trend in range condition in the arid shrub lands of Western Australia. Aust. Rangel. J. 9, 14–20.
Hu, L., Brunsell, N.A., 2013. The impact of temporal aggregation of land surface temperature data for surface urban heat island (SUHI) monitoring. Remote Sens. Environ. 134, 162–174.
Huete, A., Justice, C., Leeuwen, W.V., 1999. MODIS Vegetation Index (MOD 13),

Algorithm Theoretical Basis Document version 3, ⟨http://modis.gsfc.nasa.gov/data/atbd/atbd_mod13.pdf⟩.
Huete, A., Justice, C., Liu, H., 1994. Development of vegetation and soil indices for MODIS-EOS. Remote Sens. Environ. 49, 224–234.
Imhoff, M.L., Zhang, P., Wolfe, R.E., Bounoua, L., 2010. Remote sensing of the urban heat island effect across biomes in the continental USA. Remote Sens. Environ. 114, 504–513. http://dx.doi.org/10.1016/j.rse.2009.10.008.
Jin, M., Dickinson, R.E., Zhang, D.-L., 2005. The footprint of urban areas on global climate as characterized by MODIS. J. Clim. 18, 1551–1565.
Johnson, D.P., Stanforth, A., Lulla, V., Luber, G., 2012. Developing an applied extreme heat vulnerability index utilizing socioeconomic and environmental data. Appl. Geogr. 35 (1), 23–31.
Jonsson, P., 2004. Vegetation as an urban climate control in the subtropical city of Gaborone, Botswana. Int. J. Climatol. 24, 1307–1322.
Karl, T.R., Diaz, H.F., Kukla, G., 1988. Urbanization: Its detection and effect in the United States climate record. J. Clim. 1 (11), 1099–1123.
Khandelwal, S., Goyal, R., Kaul, N., Mathew, A., 2017. Assessment of land surface temperature variation due to change in elevation of area surrounding Jaipur, India. Egypt. J. Remote Sens. Space Sci. 21 (1), 87–94.
Klok, L., Zwart, S., Verhagen, H., Mauri, E., 2012. The surface heat island of Rotterdam and its relationship with urban surface characteristics. Resour. Conserv. Recycl. 64, 23–29.
Knapp, S., Kuhn, I., Schweiger, O., Klotz, S., 2008. Challenging urban species diversity: contrasting phylogenetic patterns across plant functional groups in Germany. Ecol. Lett. 11, 1054–1064.
Kolokotroni, M., Giridharan, R., 2008. Urban heat island intensity in London: an investigation of the impact of physical characteristics on changes in outdoor air temperature during summer. Sol. Energy 82, 986–998.
Kovats, R.S., Hajat, S., 2008. Heat stress and public health: a critical review. Annu. Rev. Public Health 29, 41–55.
Kumar, K.S., Bhaskar, P.U., K Padmakumari, K., 2012. Estimation of land surface temperature to study urban heat island effect using Landsat ETM+ image. Int. J. Eng. Sci. Technol. 4, 771–778.
Lazzarini, M., Marpu, P.M., Ghedira, H., 2012. Temperature-land cover interactions: the inversion of urban heat island phenomenon in desert city areas. Remote Sens. Environ. 130, 136–152.
Li, Y.Y., Zhang, H., Kainz, W., 2012. Monitoring patterns of urban heat islands of the fast-growing Shanghai metropolis, China: using time-series of Landsat TM/ETM+ data. Int. J. Appl. Earth Obs. Geoinf. 19, 127–138.
Liang, B.Q., Weng, Q.H., 2011. Assessing urban environmental quality change of Indianapolis (1998) United States, by the remote sensing and GIS integration. IEEEJ Sel. Top. Appl. Earth Obs. Remote Sens. 4 (1), 43–55.
Liu, L., Zhang, Y., 2011. Urban heat island analysis using the Landsat TM data and ASTER data: a case study in Hong Kong. Rem. Sens. 3, 1535–1552.
Ma, Y., Kuang, Y., Huang, N., 2010. Coupling urbanization analyses for studying urban thermal environment and its interplay with biophysical parameters based onTM/ETM + imagery. Int. J. Appl. Earth Obs. Geoinf. 12 (2), 110–118.
Mackey, C.W., Lee, X., Smith, R.B., 2012a. Remotely sensing the cooling effects of city scale efforts to reduce urban heat island. Build. Environ. 49, 348–358. http://dx.doi.org/10.1016/j.buildenv.2011.08.004.
Mackey, C.W., Lee, X., Smith, R.B., 2012b. Remotely sensing the cooling effects of city scale efforts to reduce urban heat island. Build. Environ. 49, 348–358.
Mallick, J., Singh, C.K., Shashtri, S., Rahman, A., Mukherjee, S., 2012. Land surface emissivity retrieval based on moisture index from Landsat TM satellite data over heterogeneous surfaces of Delhi city. Int. J. Appl. Earth Obs. Geoinf. 19, 348–358.
Mathew, A., Chaudhary, R., Gupta, N., Khandelwal, S., Kaul, N., 2015. Study of urban heat island effect on Ahmedabad city and its relationship with various urbanization and vegetation parameters. Int. J. Comput. Math. Sci. 4, 126–135.
Mathew, A., Khandelwal, S., Kaul, N., 2016. Spatial and temporal variations of urban heat island effect and the effect of percentage impervious surface area and elevation on land surface temperature: study of Chandigarh city, India. Sustain. Cities Soc. 26, 264–277.
Mathew, A., Khandelwal, S., Kaul, N., 2017a. Investigating spatial and seasonal variations of urban heat island effect over Jaipur city and its relationship with vegetation, urbanization and elevation parameters. Sustain. Cities Soc. 35, 157–177.
Mathew, A., Khandelwal, S., Kaul, N., 2017b. Analysis of diurnal surface temperature variations for the assessment of surface urban heat island effect over Indian cities. Energy Build. 159, 271–295.
Mathew, A., Khandelwal, S., Kaul, N., 2018. Investigating spatio-temporal surface urban heat island growth over Jaipur city using geospatial techniques. Sustain. Cities Soc. 40, 484–500.
Mirzaei, P.A., Haghighat, F., 2010. A novel approach to enhance outdoor air quality: pedestrian ventilation system. Build. Environ. 45, 1582–1593.
Oke, T.R., 1982. The energetic basis of the urban heat island. Q. J. R. Meteorol. Soc. 108, 1–24.
Owen, T., Carlson, T., Gilles, R., 1998. An assessment of satellite remotely sensed land cover parameters in quantitatively describing the climatic effect of urbanization. Int. J. Remote Sens. 19 (9), 1663–1681.
Pal, S., Ziaul, S., 2016. Detection of land use and land cover change and land surface temperature in English Bazar urban centre. Egypt. J. Remote Sens. Space Sci. 20, 125–145. http://dx.doi.org/10.1016/j.ejrs.2016.11.003.
Purevdorj, T.S., Tateishi, R., Ishiyama, T., Honda, Y., 1998. Relationships between percent vegetation cover and vegetation indices. Int. J. Rem. Sens. 19, 3519–3535.
Qiao, Z., Tian, G., Xiao, L., 2013. Diurnal and seasonal impacts of urbanization on the urban thermal environment: a case study of Beijing using MODIS data. ISPRS J. Photogramm. Remote Sens. 85, 93–101.
Rizwan, A.M., Dennis, Y.C.L., Liu, Chunho, 2008. A review on the generation, determination and mitigation of urban heat island. J. Environ. Sci. 20, 120–128.
Rotem-Mindali, O., Michael, Y., Helman, D., Lensky, I.M., 2015. The role of local land-use on the urban heat island effect of Tel Aviv as assessed from satellite remote sensing. Appl. Geogr. 56, 145–153.
Roth, M., Oke, T.R., Emery, W.J., 1989. Satellite-derived urban heat islands from three coastal cities and the utilization of such data in urban climatology. Int. J. Remote Sens. 10, 1699–1720.
Santamouris, M., Papanikolaou, N., Livada, I., Koronakis, I., Georgakis, C., Argiriou, A., Assimakopoulos, D.N., 2001. On the impact of urban climate on the energy consumption of buildings. Sol. Energy 70 (3), 201–216.
Schwarz, N., Lautenbach, S., Seppelt, R., 2011. Exploring indicators for quantifying surface urban heat islands of European cities with MODIS land surface temperatures. Remote Sens. Environ. 115 (12), 3175–3186.
Schwarz, N., Schlink, U., Franck, U., Großmann, K., 2012. Relationship of land surface and air temperatures and its implications for quantifying urban heat island indicators—An application for the city of Leipzig (Germany). Ecol. Indic. 18, 693–704.
Small, C., Elvidge, C.D., Balk, D., Montgomery, M., 2011. Spatial scaling of stable night lights. Remote Sens. Environ. 115 (2), 269–280.
Sobrino, J.A., Oltra-Carrio, R., Jimenez-Munoz, J.C., Julien, Y., Soria, G., Franch, B., Mattar, C., 2012. Emissivity mapping over urban areas using a classification-based approach: application to the Dual-use European Security IR Experiment (DESIREX). Int. J. Appl. Earth Obs. Geoinf. 18, 141–147.
Streutker, D.R., 2003. Satellite-measured growth of the urban heat island of Houston.
Taha, H., 1997. Urban climates and heat islands: albedo, evapotranspiration, and anthropogenic heat. Energy Build. 25, 99–103.
Tiangco, M., Lagmay, A.M.F., Argete, J., 2008. ASTER-based study of the night-time urban heat island effect in Metro Manila. Int. J. Remote Sens. 29 (10), 2799–2818.
Tran, H., Uchihama, D., Ochi, S., Yasuoka, Y., 2006. Assessment with satellite data of the urban heat island effects in Asian mega cities. Int. J. Appl. Earth Obs. Geoinf. 8, 34–48.
United Nations, 2010. Department of Economic and Social Affairs, Population Division. World urbanization prospects: the 2009 revision. CD-ROM Edition - Data in digital form (POP/ DB/WUP/Rev.2009).
Voogt, J.A., Oke, T.R., 2003. Thermal remote sensing of urban climates. Remote Sens. Environ. 86, 370–384.
Walsh, S.J., Moody, A., Allen, T.R., Brown, D.G., 1997. Scale dependence of NDVI and its relationship to mountainous terrain. In: Quattrochi, D.A., Goodchild, M.F. (Eds.), Scale in Remote Sensing and GIS. Lewis Publishers, Boca Raton, FL, pp. 27–55.
Weng, Q., Lu, D., Schubring, J., 2004. Estimation of land surface temperature- vegetation abundance relationship for urban heat island studies. Remote Sens. Environ. 89, 467–483.
Wilson, J.S., Clay, M., Martin, E., Stuckey, D., Vedder-Risch, K., 2003. Evaluating environmental influences of zoning in urban ecosystems with remote sensing. Remote Sens. Environ. 86 (3), 303–321.
Wu, H., Jiang, J., Zhou, J., Zhang, H., Zhang, L., Al, L., 2005. Dynamics of urban expansion in Xi'an City using Landsat TM/ETM data. Acta Geogr. Sin. 60 (1), 143–150.
Wu, H., Ye, L.P., Shi, W.Z., Clarke, K.C., 2014. Assessing the effects of land use spatial structure on urban heat islands using HJ-1B remote sensing imagery in Wuhan, China. Int. J. Appl. Earth Obs. Geoinf. 32, 67–78.
Xian, G., Crane, M., 2006. An analysis of urban thermal characteristics and associated land cover in Tampa Bay and Las Vegas using Landsat satellite data. Remote Sens. Environ. 104, 147–156.
Xiao, R., Ouyang, Z., Zheng, H., Li, W., Schienke, E., Wang, X., 2007. Spatial pattern of impervious surfaces and their impacts on land surface temperature in Beijing, China. J. Environ. Sci. 19 (2), 250–256.
Xu, H.Q., 2006. Modification of normalised difference water index (NDWI) to enhanceopen water features in remotely sensed imagery. Int. J. Remote Sens. 27, 3025–3033.
Xu, H., 2007. Extraction of urban built-up land features from landsat imagery using a thematic oriented index combination technique. Photogramm. Eng. Remote Sens. 73 (12), 1381–1391.
Yamashita, S., Sekine, K., Shoda, M., Yamashita, K., Hara, Y., 1986. On relationships between heat island and sky view factor in the cities of Tama River basin, Japan. Atmos. Environ. 20, 681–686.
Yongnian, Z., Wei, H., Benjamin, Z.F., Honghui, Z., Huimin, L., 2010. Study on the urban heat island effects and its relationship with surface biophysical characteristics using MODIS imageries. Geo-Spat. Inf. Sci. 13 (1), 1–7.
Yuan, F., Bauer, M.E., 2007. Comparison of impervious surface area and normalized difference vegetation index as indicators of surface urban heat island effects in Landsat imagery. Remote Sens. Environ. 106, 375–386.
Yue, W., Xu, J., Tan, W., Xu, L., 2007. The relationship between land surface temper-ature and NDVI with remote sensing: application to Shanghai Landsat 7 ETM+ data. Int. J. Remote Sens. 28 (15), 3205–3226.
Zha, Y., Gao, J., Ni, S., 2003. Use of normalized difference built-up index in automatically mapping urban areas from TM imagery. Int. J. Remote Sens. 24 (3), 583–594.
Zhang, H., Qi, Z.F., Ye, X.Y., Cai, Y.B., Ma, W.C., Chen, M.N., 2013. Analysis of land use/land cover change, population shift, and their effects on spatiotemporal patterns of urban heat islands in metropolitan Shanghai, China. Appl. Geogr. 44, 121–133.
Zhang, K., Wang, R., Shen, C., Da, L., 2010. Temporal and spatial characteristics of the urban heat island during rapid urbanization in Shanghai, China. Environ. Monit. Assess. 169, 101–112.
Zhang, Y., Odeh, I.O.A., Han, C., 2009. Bi-temporal characterization of land surface temperature in relation to impervious surface area, NDVI and NDBI, using sub-pixel image analysis. Int. J. Appl. Earth Obs. Geoinf. 11, 256–264.
Zhangyan, J., Yunhao, C., Jing, L., 2006. On urban heat island of Beijing based on Landsat TM data. Geo-Spat. Inf. 9 (4), 293–297.